

Numerical schemes for a multi-species quantum BGK model

Gi-Chan Bae ^{*}, Marlies Pirner [†], Sandra Warnecke [‡]

Abstract: We consider a kinetic model of an N-species gas mixture modeled with quantum Bhatnagar-Gross-Krook (BGK) collision operators. The collision operators consist of a relaxation to a Maxwell distribution in the classical case, a Fermi distribution for fermions and a Bose-Einstein distribution for bosons. In this paper we present a numerical method for simulating this model, which uses an Implicit-Explicit (IMEX) scheme to minimize a certain potential function. This is motivated by theoretical considerations coming from entropy minimization. We show that theoretical properties such as conservation of mass, total momentum and total energy as well as positivity of the distribution functions are preserved by the numerical method presented in this paper, and illustrate its usefulness and effectiveness with numerical examples

1 Introduction

In a kinetic description, the state of a dilute gas or plasma is given by a distribution function that prescribes the density of particles at each point in position-momentum phase space. In a time-dependent setting, the evolution of this distribution function is due to a balance of particle advection and binary collisions. Perhaps the most well-known model for collisions is the Boltzmann collision operator, an integral operator that preserves collision invariants (mass, momentum and energy) and dissipates the mathematical entropy of the system. Unfortunately, the expense of evaluating this operator can be prohibitive. Indeed, its evaluation requires the calculation of a five-dimensional integral at every point in phase-space. Thus even with fast spectral methods [35, 36, 16, 15], the collision operator is typically the dominant part of a kinetic calculation. The quantum modification of the celebrated Boltzmann equation was made in [39, 40] to incorporate the quantum effect that cannot be neglected for light molecules (such as Helium) at low temperature. Quantum Boltzmann equation is now fruitfully employed not just for low temperature gases, but in various circumstances such as scattering problem in solid [3, 13] and electrons on energy band structure in semiconductor [27].

In the classical case, the Bhatnagar-Gross-Krook (BGK) operator is a widely used surrogate for the Boltzmann operator that models collisions by a simple relaxation mechanism. This simplification brings significant computational advantages while also maintaining the conservation and entropy dissipation properties of the Boltzmann operator. As in the classical case, the quantum BGK models are widely used in place of the quantum Boltzmann equation [3, 13, 27, 31, 37, 32].

In the quantum case, an extension of the single-species BGK model to the multi-species setting was recently developed in [7]. There a sufficient condition is proven that guarantees the existence of equilibrium coefficients so that the model shares the same conservation laws and H-theorem with the quantum Boltzmann equation. Unlike the classical BGK model for gas mixtures [20, 25, 19, 18, 38, 28, 21, 10, 1, 11], the equilibrium coefficients of the local equilibrium for quantum multi-species gases are defined through highly nonlinear relations that are not explicitly

^{*}Seoul National University

[†]University of Muenster

[‡]University of Wuerzburg

solvable. So it was necessary to verify that such nonlinear relations uniquely determine the equilibrium coefficients, leading to the well-definedness of the model.

In this paper we present a numerical implementation of the quantum multi-species BGK model developed in [7]. The main obstacle of the quantum mixture BGK model is that the equilibrium parameters can not be written by explicit relation with mass, momentum, and energy. Here, we present a method that enables an implicit treatment of the quantum BGK operator following the recently developed method on the BGK model with velocity-dependent collision frequency [22, 23]. The implementation is a discrete velocity method that relies on standard spatial and temporal discretizations from the literature. The crucial step involves the formulation of a convex entropy minimization problem. In particular, the solver uses a numerical minimization procedure in order to determine the coefficients of the attractors. The numerical method was originally developed for a BGK model for gas mixtures with velocity dependent collision frequencies [22, 23]. In this paper, we will see that this method can be also adapted for quantum BGK models for gas mixtures since both models have structural similarities. Both models have the difficulty that the dependency of the attractors on the solution can not be given in an explicit way. The implementation is a discrete velocity method that relies on standard spatial and temporal discretizations from the literature. The key new ingredient is a solver which enables an implicit treatment of the BGK operator. The crucial step involves the formulation of a convex entropy minimization problem. In particular, the solver uses a numerical minimization procedure in order to determine the coefficients of the attractors. This construction guarantees conservation and entropy properties at the discrete level, up to numerical tolerances, even when using a discrete velocity mesh.

The remainder of this paper is organized as follows. In Section 2, 3 and 4, we recall the multi-species quantum BGK model from [7] and its main important properties. In Section 5.1, we present the first- and second-order implicit-explicit time discretizations that are used in the paper. We also introduce the optimization-based approach for the implicit evaluation of the BGK operator. In Section 5.2, we describe the space discretization. In Section 5.3, we verify some structure preserving properties of the semi-discrete scheme. In Section 5.4, we introduce the momentum discretization and summarize the numerical implementation of the optimization algorithm introduced in Section 5.1. In Section 6, we provide an array of numerical results that illustrate the properties of our scheme.

2 A consistent multi-species quantum BGK model

We consider two distribution functions $f_1 = f_1(x, p, t) \geq 0$ and $f_2 = f_2(x, p, t) \geq 0$ for species with masses $m_1 > 0$ and $m_2 > 0$, respectively, with the phase space variables (position and momentum) $x \in \Omega$ and $p \in \mathbb{R}^3$ and time $t \geq 0$. To be as general as possible, we generalize the quantum mixture BGK model in [7] describing a mixture of bosons and fermions to the mixture of gases including the interaction of quantum-classical particles:

$$\begin{aligned} \partial_t f_1 + \frac{p}{m_1} \cdot \nabla_x f_1 &= \nu_{11} n_1 (\mathcal{K}_{11} - f_1) + \nu_{12} n_2 (\mathcal{K}_{12} - f_1), \\ \partial_t f_2 + \frac{p}{m_2} \cdot \nabla_x f_2 &= \nu_{22} n_2 (\mathcal{K}_{22} - f_2) + \nu_{21} n_1 (\mathcal{K}_{21} - f_2), \end{aligned} \tag{1}$$

where \mathcal{K}_{ij} is the local equilibrium describing the interactions of i th and j th component and $\nu_{ij} n_j$ for $i, j = 1, 2$ are the collision frequencies. More explicitly, there can be the following cases for fermion $\tau = +1$, for boson $\tau = -1$, and for classical particle $\tau = 0$:

$$\begin{aligned} \mathcal{K}_{11} &= \frac{1}{e^{m_1 a_1 \left| \frac{p}{m_1} - b_1 \right|^2 + c_1} + \tau}, & \mathcal{K}_{12} &= \frac{1}{e^{m_1 a \left| \frac{p}{m_1} - b \right|^2 + c_{12}} + \tau}, \\ \mathcal{K}_{22} &= \frac{1}{e^{m_2 a_2 \left| \frac{p}{m_2} - b_2 \right|^2 + c_2} + \tau'}, & \mathcal{K}_{21} &= \frac{1}{e^{m_2 a \left| \frac{p}{m_2} - b \right|^2 + c_{21}} + \tau'}. \end{aligned} \tag{2}$$

We denote \mathcal{K} as Fermi-Dirac distribution, Bose-Einstein distribution and Maxwellian for the case $\tau = +1, -1, 0$, respectively. The equilibrium parameters (a_i, b_i, c_i) and (a, b, c_{12}, c_{21}) will be determined later to satisfy the conservation laws and the entropy principle. Note that the model includes the following cases depending on the types of the particles

$$(\tau, \tau') = \begin{cases} (+1, +1) & \text{(fermion-fermion)} \\ (-1, -1) & \text{(boson-boson)} \\ (+1, -1) & \text{(fermion-boson)} \\ (+1, 0) & \text{(fermion-classical)} \\ (0, -1) & \text{(classical-boson)} \\ (0, 0) & \text{(classical-classical)} \end{cases}$$

We define the number density of particles n_i , momentum P_i , energy E_i of each species as

$$n_i = \int_{\mathbb{R}^3} f_i dp, \quad P_i = \int_{\mathbb{R}^3} f_i p dp, \quad E_i = \int_{\mathbb{R}^3} f_i \frac{|p|^2}{2m_i} dp, \quad (3)$$

and $m_i n_i = N_i$. The parameters (a_i, b_i, c_i) in \mathcal{K}_{ii} are chosen such that the local equilibrium satisfies the following identities:

$$\int_{\mathbb{R}^3} \mathcal{K}_{ii} dp = n_i, \quad \int_{\mathbb{R}^3} \mathcal{K}_{ii} p dp = P_i, \quad \int_{\mathbb{R}^3} \mathcal{K}_{ii} \frac{|p|^2}{2m_i} dp = E_i, \quad (i = 1, 2). \quad (4)$$

This ensures conservation of the number of particles, momentum and energy in interactions of a species with itself.

The equilibrium parameters (a, b, c_{12}, c_{21}) of \mathcal{K}_{ij} for $(ij) = (12), (21)$ are determined to satisfy the following identities:

$$\begin{aligned} \int_{\mathbb{R}^3} \mathcal{K}_{12} dp &= n_1, & \int_{\mathbb{R}^3} \mathcal{K}_{21} dp &= n_2, \\ \nu_{12} n_2 \left(\int_{\mathbb{R}^3} \mathcal{K}_{12} p dp - P_1 \right) + \nu_{21} n_1 \left(\int_{\mathbb{R}^3} \mathcal{K}_{21} p dp - P_2 \right) &= 0, \\ \nu_{12} n_2 \left(\int_{\mathbb{R}^3} \mathcal{K}_{12} \frac{|p|^2}{2m_1} dp - E_1 \right) + \nu_{21} n_1 \left(\int_{\mathbb{R}^3} \mathcal{K}_{21} \frac{|p|^2}{2m_2} dp - E_2 \right) &= 0. \end{aligned} \quad (5)$$

This ensures conservation of the number of particles, momentum and energy in interactions of a species with the other one.

The existence of these parameters (a_i, b_i, c_i) and (a, b, c_{12}, c_{21}) is proven in [7] for quantum-quantum mixture case with unit collision frequencies. We will show the proof for any choice of mixture between classical particle, fermion, and boson for more general collision frequency the correspondence with the classical case.

Remark 1. For the correspondence of classical case and quantum case, let us assume that the velocity distribution function $\bar{f}_i(x, v, t)$ and the momentum distribution function $f_i(x, p, t)$ satisfy the following relation for $(i = 1, 2)$:

$$\bar{f}_i(x, v, t) = \bar{f}_i\left(x, \frac{p}{m_i}, t\right) = m_i^3 f_i(x, p, t).$$

This relation connects the conservation laws of classical case and quantum case as follows:

$$\int_{\mathbb{R}^3} \bar{f}_i(x, v, t) \begin{pmatrix} 1 \\ m_i v \\ \frac{m_i}{2} |v|^2 \end{pmatrix} dv = \int_{\mathbb{R}^3} \frac{1}{m_i^3} \bar{f}_i\left(x, \frac{p}{m_i}, t\right) \begin{pmatrix} 1 \\ p \\ \frac{|p|^2}{2m_i} \end{pmatrix} dp = \int_{\mathbb{R}^3} f_i(x, p, t) \begin{pmatrix} 1 \\ p \\ \frac{|p|^2}{2m_i} \end{pmatrix} dp.$$

Thus the macroscopic fields of the classical one

$$\begin{aligned} n_i(x, t) &= \int_{\mathbb{R}^3} \bar{f}_i(x, v, t) dv, \quad m_i n_i = \rho_i \\ U_i(x, t) &= \frac{1}{n_i} \int_{\mathbb{R}^3} \bar{f}_i(x, v, t) v dv, \\ T_i(x, t) &= \frac{1}{3n_i} \int_{\mathbb{R}^3} \bar{f}_i(x, v, t) m_i |v - U_i|^2 dv, \end{aligned}$$

and the quantum one

$$\begin{aligned} n_i(x, t) &= \int_{\mathbb{R}^3} f_i(x, p, t) dp, \quad m_i n_i = N_i \\ P_i(x, t) &= \int_{\mathbb{R}^3} f_i(x, p, t) p dp, \\ E_i(x, t) &= \int_{\mathbb{R}^3} f_i(x, p, t) \frac{|p|^2}{2m_i} dp, \end{aligned}$$

have the following relation:

$$\begin{aligned} \rho_i &= m_i \int_{\mathbb{R}^3} \bar{f} dv = m_i \int_{\mathbb{R}^3} f dp = N_i, \\ \rho_i U_i &= m_i \int_{\mathbb{R}^3} \bar{f} v dv = \int_{\mathbb{R}^3} f p dp = P_i, \\ \frac{3}{2} n_i T_i + \frac{1}{2} \rho_i |U_i|^2 &= \int_{\mathbb{R}^3} \bar{f} \frac{m_i}{2} |v|^2 dv = \int_{\mathbb{R}^3} f \frac{|p|^2}{2m_i} dp = E_i. \end{aligned} \tag{6}$$

Having introduced our notation, we can deep dive into the model [7].

3 Properties of the model

In this section, we present the main properties of the quantum multi-species BGK model (1).

3.1 Conservation properties, H-Theorem and Boundedness

First of all, the model satisfies the conservation properties and an H -Theorem if the macroscopic fields have some boundedness conditions. This is already proved in [7] for the Fermion-Fermion, Fermion-Boson and Boson-Boson case with collision frequency $\nu_{ij} n_j = 1, i, j = 1, 2$. We generalize the result to include the Fermion-classical, Boson-classical and classical-classical case with (x, t) depending general collision frequency $\nu_{ij} n_j$.

One of the most characterizing features of quantum mechanics is that the number of particles cannot exceed the specific ratio of the energy. If the number of particles exceeds that critical point, then Bose-Einstein condensation occurs for bosons or saturated state occurs for fermions. Consequently, the local equilibrium of the one-species quantum BGK model is only defined below the specific ratio between number of particles and energy (see [12, 4, 29, 30]). Hence

we introduce the function j_τ by

$$j_\tau(x) = \frac{\int \frac{1}{e^{|p|^2+x+\tau}} dp}{\left(\int \frac{|p|^2}{e^{|p|^2+x+\tau}} dp\right)^{3/5}}.$$

In the following, we will describe how the equilibrium parameters (a_i, b_i, c_i) and (c_{12}, c_{21}, a, b) in (2) will be determined in order to ensure the conservation properties (4) and (5). We start with the equilibrium parameters in the one-species term. The equilibrium parameter c_i is uniquely determined by the following implicit relation,

$$j_\tau(c_i) = \frac{n_i}{(2m_i E_i - |P_i|^2/n_i)^{3/5}},$$

if the right-hand-side is bounded as follows:

$$\frac{n_i}{(2m_i E_i - |P_i|^2/n_i)^{3/5}} \leq \begin{cases} j_{+1}(-\infty) & \text{for fermion,} \\ j_{-1}(0) & \text{for boson.} \end{cases}$$

(with notation $j_{+1}(-\infty) = \lim_{x \rightarrow -\infty} j_{+1}(x)$. The reason is that the functions j_{+1} and j_{-1} are strictly decreasing on $(-\infty, \infty)$ and $[0, \infty)$, respectively).

In the classical case, we can explicitly compute $j_0(x) = \left(\frac{2\pi}{3}\right)^{3/5} e^{-\frac{2}{5}x}$, which is strictly decreasing. Thus the maximum value of $j_0(x)$ is equal to $\lim_{x \rightarrow -\infty} j_0(x) = \infty$, and the macroscopic fields of the classical case has no restriction from above:

$$0 \leq \frac{n_i}{(2m_i E_i - |P_i|^2/n_i)^{3/5}} < \infty.$$

We define l_{+1}, l_0 and l_{-1} to be such points where the respective functions j_{+1}, j_0 and j_{-1} are maximal and use the following notation

$$l : \{+1, -1, 0\} \rightarrow [-\infty, \infty], \quad l_\tau = \begin{cases} l_{+1} = -\infty, \\ l_{-1} = 0, \\ l_0 = -\infty. \end{cases}$$

Then, if the specific ratio of macroscopic fields has the following bound

$$\frac{n_i}{(2m_i E_i - |P_i|^2/n_i)^{3/5}} \leq j_\tau(l_\tau),$$

then the equilibrium parameter c_i is uniquely determined by

$$c_i = j_\tau^{-1} \left(\frac{n_i}{(2m_i E_i - |P_i|^2/n_i)^{3/5}} \right).$$

Finally, we can define a_i , and b_i by

$$a_i = \left(\int_{\mathbb{R}^3} \frac{1}{e^{|p|^2+c_i+\tau}} dp \right)^{2/3} n_i^{-2/3}, \quad b_i = \frac{P_i}{n_i}, \quad (7)$$

for $(i = 1, 2)$. This choice ensures the conservation properties (4) and is proven in [4]. To summarize, we have the following theorem.

Theorem 3.1.1. *Let the macroscopic fields satisfy*

$$\frac{n_1}{(2m_1E_1 - |P_1|^2/n_1)^{\frac{3}{5}}} \leq j_\tau(l(\tau)), \quad \frac{n_2}{(2m_2E_2 - |P_2|^2/n_2)^{\frac{3}{5}}} \leq j_{\tau'}(l(\tau')).$$

Then the parameters of \mathcal{K}_{11} and \mathcal{K}_{22} are uniquely determined as

$$c_1 = j_\tau^{-1} \left(\frac{n_1}{(2m_1E_1 - |P_1|^2/n_1)^{\frac{3}{5}}} \right), \quad c_2 = j_{\tau'}^{-1} \left(\frac{n_2}{(2m_2E_2 - |P_2|^2/n_2)^{\frac{3}{5}}} \right).$$

and

$$a_1 = \left(\int_{\mathbb{R}^3} \frac{1}{e^{|p|^2+c_1} + \tau} dp \right)^{\frac{2}{3}} n_1^{-\frac{2}{3}}, \quad a_2 = \left(\int_{\mathbb{R}^3} \frac{1}{e^{|p|^2+c_2} + \tau'} dp \right)^{\frac{2}{3}} n_2^{-\frac{2}{3}},$$

and

$$b_1 = \frac{P_1}{n_1}, \quad b_2 = \frac{P_2}{n_2}.$$

Then with this choice of the equilibrium parameters of the one species quantum equilibrium \mathcal{K}_{11} and \mathcal{K}_{22} the conservation properties (4) are satisfied.

We note that the local Maxwellian for the classical case corresponds to the original definition in [9]:

$$\mathcal{M}_{ii} = \frac{N_i}{\pi^{\frac{3}{2}}} \left(\frac{3}{2} \frac{1}{\frac{E_i}{N_i} - \left| \frac{P_i}{N_i} \right|^2} \right)^{\frac{3}{2}} e^{-\frac{3}{2} \frac{\left| p - \frac{P_i}{N_i} \right|^2}{\frac{E_i}{N_i} - \left| \frac{P_i}{N_i} \right|^2}} = \frac{n_i}{\sqrt{2\pi} \frac{T_i}{m_i}} \exp \left(-\frac{|v - U_i|^2}{2 \frac{T_i}{m_i}} \right),$$

where we applied the correspondence of the macroscopic fields (6). Then we can see that with such choice of a_i , b_i and c_i , the local equilibria $\mathcal{K}_{11} = \mathcal{M}_{11}$ and $\mathcal{K}_{22} = \mathcal{M}_{22}$ satisfy (4).

Before stating the theorem for the mixture interaction terms, we introduce some notations. We define

$$\eta_\tau(x) = \int_{\mathbb{R}^3} \frac{1}{e^{|p|^2+x} + \tau} dp.$$

Note that η_τ^{-1} always exist since η_τ is strictly decreasing. We define $k_{\tau,\tau'}$ by

$$k_{\tau,\tau'}(x, y) = \frac{m_1^{3/2} \int_{\mathbb{R}^3} \frac{1}{e^{|p|^2+x} + \tau} dp}{\left(\frac{\nu_{12}}{m_2} \left(\frac{m_1^{3/2}}{2N_1} \int_{\mathbb{R}^3} \frac{|p|^2}{e^{|p|^2+x} + \tau} dp \right) + \frac{\nu_{21}}{m_1} \left(\frac{m_2^{3/2}}{2N_2} \int_{\mathbb{R}^3} \frac{|p|^2}{e^{|p|^2+y} + \tau'} dp \right) \right)^{\frac{3}{5}}}.$$

Using η_τ and k_τ , we define $g_{\tau,\tau'}$, which is defined as a composite function of k_τ and η_τ^{-1} , as follows:

$$g_{\tau,\tau'}(x) = k_{\tau,\tau'}(x, y(x)) = \frac{m_1^{3/2} \int_{\mathbb{R}^3} \frac{1}{e^{|p|^2+x} + \tau} dp}{\left(\frac{\nu_{12}}{m_2} \left(\frac{m_1^{3/2}}{2N_1} \int_{\mathbb{R}^3} \frac{|p|^2}{e^{|p|^2+x} + \tau} dp \right) + \frac{\nu_{21}}{m_1} \left(\frac{m_2^{3/2}}{2N_2} \int_{\mathbb{R}^3} \frac{|p|^2}{e^{|p|^2+y(x)} + \tau'} dp \right) \right)^{\frac{3}{5}}}, \quad (8)$$

where $y(x)$ denotes

$$y(x) = \eta_\tau^{-1} \left(\frac{m_1^{3/2} n_2}{m_2^{3/2} n_1} \eta_\tau(x) \right).$$

Theorem 3.1.2. Assume $\nu_{12}n_2 = \nu_{21}n_1$. Assume further that

$$\frac{n_1}{\left(2E_1 + 2E_2 - \frac{|P_1+P_2|^2}{N_1+N_2}\right)^{\frac{3}{5}}} \leq g_{\tau,\tau'} \left(\max \left\{ l(\tau), h_{\tau}^{-1} \left(\frac{m_2^{\frac{3}{2}}n_1}{m_1^{\frac{3}{2}}n_2} h_{\tau'}(l(\tau')) \right) \right\} \right).$$

Then c_{12}, c_{21} are defined as a unique solution of the following relations:

$$\frac{m_1^{\frac{3}{2}}h_{\tau}(c_{12})}{m_2^{\frac{3}{2}}h_{\tau'}(c_{21})} = \frac{n_1}{n_2}, \quad k_{\tau,\tau'}(c_{12}, c_{21}) = \frac{n_1}{\left(2E_1 + 2E_2 - \frac{|P_1+P_2|^2}{N_1+N_2}\right)^{\frac{3}{5}}}. \quad (9)$$

With such c_{12} and c_{21} , we define a and b by

$$a = \left(\frac{m_1^{\frac{3}{2}} \int_{\mathbb{R}^3} \frac{|p|^2}{e^{|p|^2+c_{12}+\tau}} dp + m_2^{\frac{3}{2}} \int_{\mathbb{R}^3} \frac{|p|^2}{e^{|p|^2+c_{21}+\tau'}} dp \right)^{\frac{2}{5}}, \quad b = \frac{P_1 + P_2}{N_1 + N_2}, \quad (10)$$

Then with this choice of the equilibrium parameters of the mixture species quantum equilibrium \mathcal{K}_{12} and \mathcal{K}_{21} the conservation properties (5) are satisfied.

Another property of the model is that the distribution function in the fermion case remains bounded from above by 1 for all times $t \geq 0$. The proof can be found in [7].

Lemma 3.1.3. Let f_i be a distribution function for fermions and $f_i(x, p, 0) < 1$. Then we have $f_i(x, p, t) < 1$ for $t \geq 0$.

Now we consider the entropy principle. For the convenience of notation, we denote

$$H_{\tau}(f) = \begin{cases} \int_{\Omega} \int_{\mathbb{R}^3} f \ln f dp dx & \text{for } \tau = 0 \\ \int_{\Omega} \int_{\mathbb{R}^3} f \ln f + \tau^{-1}(1 - \tau f) \ln(1 - \tau f) dp dx & \text{for } \tau = \pm 1 \end{cases}$$

($\tau = +1$ for fermion, $\tau = -1$, for boson) By abusing the notation $\lim_{\tau \rightarrow 0^+} \tau^{-1}(1 - \tau f) \ln(1 - \tau f) = 0$, we also denote the integrand by h_{τ} , namely

$$h_{\tau}(z) = z \ln z + \tau^{-1}(1 - \tau z) \ln(1 - \tau z) \quad (11)$$

for $z > 0$ if $\tau = 0, -1$ and $0 < z < 1$ if $\tau = +1$. Then, we define the entropy for the gas mixture as follows:

$$H_{\tau,\tau'}(f_1, f_2) = H_{\tau}(f_1) + H_{\tau'}(f_2)$$

The function $H_{\tau,\tau'}$ can be proven to be a non-increasing function for the model (1).

Theorem 3.1.4. Let (f_1, f_2) be a solution of the equation (1). If the i -th component is a fermion, we give an additional assumption that $f_i < 1$. Then we have

$$\frac{d}{dt} H_{\tau,\tau'}(f_1, f_2) \leq 0.$$

The equality is characterized by f_1 and f_2 being two Fermion distributions in the Fermion-Fermion case, two Boson distributions in the Boson-Boson case, two Maxwell distributions in the classical-classical case, a Fermi distribution and a Bose distribution in the Fermion-Boson case, a Fermi distribution and a Maxwell distribution in the Fermion-classical case and a Bose distribution and a Maxwell distribution in the Bose-classical case. In all cases, these equilibrium distributions have the same a and b .

The proof is a straightforward extension of the proof of Theorem 2.1(3) in [7].

3.2 Macroscopic equations

From the quantum BGK model (1), one can derive the macroscopic equations for a mixture. We first denote the macroscopic fields of the inter-species local equilibrium \mathcal{K}_{12} and \mathcal{K}_{21} :

$$\begin{aligned} P_{12} &= \int_{\mathbb{R}^3} \mathcal{K}_{12} p dp, & P_{21} &= \int_{\mathbb{R}^3} \mathcal{K}_{21} p dp, \\ E_{12} &= \int_{\mathbb{R}^3} \mathcal{K}_{12} \frac{|p|^2}{2m_1} dp, & E_{21} &= \int_{\mathbb{R}^3} \mathcal{K}_{12} \frac{|p|^2}{2m_2} dp. \end{aligned} \quad (12)$$

Theorem 3.2.1. *Assume $\nu_{12}n_1 = \nu_{21}n_2$. Let (f_1, f_2) be a solution to (1), then we obtain the following formal conservation laws*

$$\begin{aligned} \partial_t n_1 + \frac{1}{m_1} \nabla_x \cdot P_1 &= 0, & \partial_t n_2 + \frac{1}{m_2} \nabla_x \cdot P_2 &= 0, \\ \partial_t P_1 + \frac{1}{m_1} \nabla_x \cdot \int p \otimes p f_1 dp &= \nu_{12} n_2 (P_{12} - P_1) \\ \partial_t P_2 + \frac{1}{m_2} \nabla_x \cdot \int p \otimes p f_1 dp &= \nu_{21} n_1 (P_{21} - P_2) \\ \partial_t E_1 + \frac{1}{2m_1^2} \nabla_x \cdot \int |p|^2 p f_1 dp &= \nu_{12} n_2 (E_{12} - E_1), \\ \partial_t E_2 + \frac{1}{2m_2^2} \nabla_x \cdot \int |p|^2 p f_2 dp &= \nu_{21} n_1 (E_{21} - E_2), \end{aligned} \quad (13)$$

where the exchange terms of momentum can be computed as

$$P_{12} - P_1 = -(P_{21} - P_2) = \frac{N_1 N_2}{N_1 + N_2} \left(\frac{P_2}{N_2} - \frac{P_1}{N_1} \right) \quad (14)$$

Furthermore, we define the function $\eta_\tau^E(c) = \int \frac{|p|^2}{e^{|p|^2 + c + \tau}} dp$, and obtain for the exchange of energy

$$\begin{aligned} E_{12} - E_1 &= -(E_{21} - E_2) \\ &= \frac{1}{2} \frac{N_1 |P_1 + P_2|^2}{(N_1 + N_2)^2} + \frac{(E_1 + E_2) - \frac{1}{2} \frac{|P_1 + P_2|^2}{N_1 + N_2}}{m_1^{3/2} \eta_\tau^E(c_{12}) + m_2^{3/2} \eta_\tau^E(c_{21})} m_1^{3/2} \eta_\tau^E(c_{12}) - E_1 \end{aligned} \quad (15)$$

Proof. We multiply the first equation of (1) by $(1, p, \frac{|p|^2}{2m_1})$, and the second one by $(1, p, \frac{|p|^2}{2m_2})$. Then we integrate them with respect to the momentum p to obtain (13) after a straight-forward computation on the left-hand side.

The exchange of momentum can be computed as follows. After computing the integral in the definition of P_{12} and P_{21} in (12), we observe that $P_{12} = bN_1$ and $P_{21} = bN_2$. Substituting the quantity of b in (10), we obtain

$$\frac{P_{12}}{N_1} - \frac{P_1}{N_1} = \frac{P_1 + P_2}{N_1 + N_2} - \frac{P_1}{N_1} = \frac{N_2}{N_1 + N_2} \left(\frac{P_2}{N_2} - \frac{P_1}{N_1} \right),$$

and

$$\frac{P_{21}}{N_2} - \frac{P_2}{N_2} = \frac{P_1 + P_2}{N_1 + N_2} - \frac{P_2}{N_2} = \frac{N_1}{N_1 + N_2} \left(\frac{P_1}{N_1} - \frac{P_2}{N_2} \right).$$

Then, we can compute (similar as in section 2 in [4])

$$E_{12} - \frac{1}{2} \frac{|P_{12}|^2}{N_1} = \frac{1}{2} a^{-5/2} m_1^{3/2} \eta_\tau^E(c_{12}) \quad (16)$$

We can replace $a^{-5/2}$ with the formula (10):

$$E_{12} - \frac{1}{2} \frac{|P_{12}|^2}{N_1} = \frac{(E_1 + E_2) - \frac{1}{2} \frac{|P_1 + P_2|^2}{N_1 + N_2}}{m_1^{3/2} \eta_\tau^E(c_{12}) + m_2^{3/2} \eta_{\tau'}^E(c_{21})} m_1^{3/2} \eta_\tau^E(c_{12})$$

So we obtain

$$\begin{aligned} E_{12} - E_1 &= -(E_{21} - E_2) \\ &= \frac{1}{2} \frac{N_1 |P_1 + P_2|^2}{(N_1 + N_2)^2} + \frac{(E_1 + E_2) - \frac{1}{2} \frac{|P_1 + P_2|^2}{N_1 + N_2}}{m_1^{3/2} \eta_\tau^E(c_{12}) + m_2^{3/2} \eta_{\tau'}^E(c_{21})} m_1^{3/2} \eta_\tau^E(c_{12}) - E_1 \end{aligned} \quad (17)$$

□

Remark 2. For later purposes, we remark that in the space-homogeneous case the system of equations reduces to

$$\begin{aligned} \partial_t n_1 &= 0, & \partial_t n_2 &= 0, \\ \partial_t P_1 &= \nu_{12} n_2 (P_{12} - P_1), & \partial_t P_2 &= \nu_{21} n_1 (P_{21} - P_2), \\ \partial_t E_1 &= \nu_{12} n_2 (E_{12} - E_1), & \partial_t E_2 &= \nu_{21} n_1 (E_{21} - E_2). \end{aligned} \quad (18)$$

Remark 3. In the classical case ($\tau = \tau' = 0$) we get from the relationship (9)

$$\frac{n_1}{n_2} = \frac{m_1^{3/2} \eta_0(c_{12})}{m_2^{3/2} \eta_0(c_{21})} = \frac{m_1^{3/2} \int_{\mathbb{R}^3} \frac{1}{e^{|p|^2 + c_{12}}} dp}{m_2^{3/2} \int_{\mathbb{R}^3} \frac{1}{e^{|p|^2 + c_{21}}} dp} = \frac{m_1^{3/2} e^{-c_{12}}}{m_2^{3/2} e^{-c_{21}}}$$

by computing the integrals explicitly. Using this, we can calculate

$$\frac{m_1^{3/2} \eta_0^E(c_{12})}{m_1^{3/2} \eta_0^E(c_{12}) + m_2^{3/2} \eta_0^E(c_{21})} = \frac{m_1^{3/2} e^{-c_{12}}}{m_1^{3/2} e^{-c_{12}} + m_2^{3/2} e^{-c_{21}}} = \frac{n_1}{n_1 + n_2}$$

and obtain

$$\begin{aligned} E_{12} - E_1 &= \frac{n_1 n_2}{n_1 + n_2} \left(\frac{E_2}{n_2} - \frac{E_1}{n_1} + \frac{m_1 - m_2}{(N_1 + N_2)^2} \frac{1}{2} |P_1 + P_2|^2 \right) \\ &= \frac{n_1 n_2}{n_1 + n_2} \left(\frac{E_2}{n_2} - \frac{1}{2} \frac{|P_2|^2}{n_2 N_2} - \frac{E_1}{n_1} + \frac{|P_1|^2}{n_1 N_1} + m_1 m_2 \frac{n_1 N_1 + 2n_1 N_2 + n_2 N_2}{(N_1 + N_2)^2} \frac{1}{2} \frac{|P_2|^2}{N_2^2} \right. \\ &\quad \left. - m_1 m_2 \frac{n_1 N_1 + 2N_1 n_2 + n_2 N_2}{(N_1 + N_2)^2} \frac{1}{2} \frac{|P_1|^2}{N_1^2} + m_1 m_2 \frac{(m_1 - m_2) n_1 n_2}{(N_1 + N_2)^2} \frac{P_1}{N_1} \cdot \frac{P_2}{N_2} \right) \\ &= \frac{n_1 n_2}{n_1 + n_2} \left(\frac{E_2}{n_2} - \frac{1}{2} \frac{|P_2|^2}{n_2 N_2} - \frac{E_1}{n_1} + \frac{|P_1|^2}{n_1 N_1} + m_1 m_2 \frac{n_1 N_1 + n_2 N_2}{(N_1 + N_2)^2} \frac{1}{2} \left(\frac{|P_2|^2}{N_2^2} - \frac{|P_1|^2}{N_1^2} \right) \right. \\ &\quad \left. + \left(\frac{P_2}{N_2} - \frac{P_1}{N_1} \right) \cdot \left(\frac{P_1}{n_1} + \frac{P_2}{n_2} \right) \right). \end{aligned}$$

3.3 Decay rate for the velocities and kinetic temperatures in the space-homogeneous case

In equilibrium, both distribution functions f_1 and f_2 will finally share the same velocity and the same temperature. We can make those decay rates explicit in the space-homogeneous case.

Theorem 3.3.1. *Assume $\nu_{12}n_1 = \nu_{21}n_2$ and ν_{12}, ν_{21} independent of t . In the space-homogeneous case of (1), we have the following convergence rate for the momentum*

$$\frac{P_1}{N_1} - \frac{P_2}{N_2} = e^{-\frac{\nu_{12}n_2N_2 + \nu_{21}n_1N_1}{N_1 + N_2}t} \left(\frac{P_1(0)}{N_1} - \frac{P_2(0)}{N_2} \right). \quad (19)$$

Proof. We start with calculating

$$\partial_t \left(\frac{P_1}{N_1} \right) = \frac{1}{N_1} \partial_t P_1 = \nu_{12}n_2 \frac{1}{N_1} (P_{12} - P_1).$$

The first equality uses that $N_1 = m_1n_1$ is constant in the space-homogeneous case (18). Then, we used the macroscopic equation for the time evolution of P_1 from (18) Using the expression (14) for the exchange of momentum leads to

$$\partial_t \left(\frac{P_1}{N_1} \right) = \nu_{12}n_2 \frac{N_2}{N_1 + N_2} \left(\frac{P_2}{N_2} - \frac{P_1}{N_1} \right). \quad (20)$$

In a similar way, we can compute

$$\partial_t \left(\frac{P_2}{N_2} \right) = \nu_{21}n_1 \frac{N_1}{N_1 + N_2} \left(\frac{P_1}{N_1} - \frac{P_2}{N_2} \right).$$

If we subtract the two equations we obtain

$$\partial_t \left(\frac{P_1}{N_1} - \frac{P_2}{N_2} \right) = -\frac{\nu_{12}n_2N_2 + \nu_{21}n_1N_1}{N_1 + N_2} \left(\frac{P_1}{N_1} - \frac{P_2}{N_2} \right)$$

It follows the result

$$\frac{P_1}{N_1} - \frac{P_2}{N_2} = e^{-\frac{\nu_{12}n_2N_2 + \nu_{21}n_1N_1}{N_1 + N_2}t} \left(\frac{P_1(0)}{N_1} - \frac{P_2(0)}{N_2} \right).$$

□

Remark 4. *Using the relationship $P_j = N_j b_j$ from (7), one can equivalently write*

$$b_1 - b_2 = e^{-\frac{\nu_{12}n_1N_2 + \nu_{21}n_2N_1}{N_1 + N_2}t} (b_1(0) - b_2(0)).$$

We continue with the convergence rates of the quantities $\frac{E_1}{n_1} - \frac{1}{2} \frac{|P_1|^2}{n_1 N_1}$ and $\frac{E_2}{n_2} - \frac{1}{2} \frac{|P_2|^2}{n_2 N_2}$. In the classical case, this quantity corresponds to the temperature.

Theorem 3.3.2. Let $\nu_{12}n_1 = \nu_{21}n_2 =: \tilde{\nu}$ and $\tilde{\nu}$ be independent of t . In the space-homogeneous case of (1), it is

$$\begin{aligned}
& \left(\frac{E_1}{n_1} - \frac{1}{2} \frac{|P_1|^2}{n_1 N_1} \right) - \left(\frac{E_2}{n_2} - \frac{1}{2} \frac{|P_2|^2}{n_2 N_2} \right) \\
&= e^{-\tilde{\nu}t} \left(\left(\frac{E_1(0)}{n_1} - \frac{1}{2} \frac{|P_1(0)|^2}{n_1 N_1} \right) - \left(\frac{E_2(0)}{n_2} - \frac{1}{2} \frac{|P_2(0)|^2}{n_2 N_2} \right) \right) + \frac{1}{2} m_1 m_2 \frac{n_2 N_2 - n_1 N_1}{(N_1 + N_2)^2} e^{-\tilde{\nu}t} (1 - e^{-\tilde{\nu}t}) \left| \frac{P_2(0)}{N_2} - \frac{P_1(0)}{N_1} \right|^2 \\
&+ \left(E_1(0) + E_2(0) - \frac{1}{2} \frac{|P_1(0) + P_2(0)|^2}{N_1 + N_2} \right) e^{-\tilde{\nu}t} \int_0^t e^{\tilde{\nu}s} \left[\frac{\frac{m_1^{3/2} H_\tau^E(c_{12}(s))}{n_1} - \frac{m_2^{3/2} H_{\tau'}^E(c_{21}(s))}{n_2}}{m_1^{3/2} H_\tau^E(c_{12}) + m_2^{3/2} H_{\tau'}^E(c_{21})} \right] ds.
\end{aligned} \tag{21}$$

Proof. We compute

$$\partial_t \left(\frac{E_1}{n_1} - \frac{1}{2} \frac{|P_1|^2}{n_1 N_1} \right) = \frac{1}{n_1} \partial_t (E_1) - \frac{P_1}{n_1} \partial_t \left(\frac{P_1}{N_1} \right) = \tilde{\nu} \left(\frac{E_{12}}{n_1} - \frac{E_1}{n_1} - \frac{P_1}{n_1} \frac{N_2}{N_1 + N_2} \left(\frac{P_2}{N_2} - \frac{P_1}{N_1} \right) \right). \tag{22}$$

using that n_1 is constant in the space-homogeneous case, equation (18) and inserting (20).

Applying (17), it follows

$$\begin{aligned}
& \partial_t \left(\frac{E_1}{n_1} - \frac{1}{2} \frac{|P_1|^2}{n_1 N_1} \right) \\
&= \tilde{\nu} \left(\frac{1}{2} \frac{m_1 |P_1 + P_2|^2}{(N_1 + N_2)^2} + \frac{(E_1 + E_2) - \frac{1}{2} \frac{|P_1 + P_2|^2}{N_1 + N_2}}{m_1^{3/2} H_\tau^E(c_{12}) + m_2^{3/2} H_{\tau'}^E(c_{21})} \frac{m_1^{3/2} H_\tau^E(c_{12})}{n_1} - \frac{E_1}{n_1} - \frac{P_1}{n_1} \frac{N_2}{N_1 + N_2} \left(\frac{P_2}{N_2} - \frac{P_1}{N_1} \right) \right).
\end{aligned} \tag{23}$$

Analogously for species 2 we obtain

$$\begin{aligned}
& \partial_t \left(\frac{E_2}{n_2} - \frac{1}{2} \frac{|P_2|^2}{n_2 N_2} \right) \\
&= \tilde{\nu} \left(\frac{1}{2} \frac{m_2 |P_1 + P_2|^2}{(N_1 + N_2)^2} + \frac{(E_1 + E_2) - \frac{1}{2} \frac{|P_1 + P_2|^2}{N_1 + N_2}}{m_1^{3/2} H_\tau^E(c_{12}) + m_2^{3/2} H_{\tau'}^E(c_{21})} \frac{m_2^{3/2} H_{\tau'}^E(c_{21})}{n_2} - \frac{E_2}{n_2} - \frac{P_2}{n_2} \frac{N_1}{N_1 + N_2} \left(\frac{P_1}{N_1} - \frac{P_2}{N_2} \right) \right).
\end{aligned}$$

Subtracting both, we get

$$\begin{aligned}
& \partial_t \left(\left(\frac{E_1}{n_1} - \frac{1}{2} \frac{|P_1|^2}{n_1 N_1} \right) - \left(\frac{E_2}{n_2} - \frac{|P_2|^2}{n_2 N_2} \right) \right) \\
&= \tilde{\nu} \left(\frac{E_2}{n_2} - \frac{E_1}{n_1} + \frac{\frac{1}{2}(m_1 - m_2)n_1 N_1 + N_2(N_1 + N_2)}{(N_1 + N_2)^2} \frac{|P_1|^2}{n_1 N_1} + \frac{\frac{1}{2}(m_1 - m_2)n_2 N_2 - N_1(N_1 + N_2)}{(N_1 + N_2)^2} \frac{|P_2|^2}{n_2 N_2} \right. \\
&\quad \left. + \frac{(n_1 N_1 - n_2 N_2)}{(N_1 + N_2)^2 n_1 n_2} P_1 \cdot P_2 + \frac{(E_1 + E_2) - \frac{1}{2} \frac{|P_1 + P_2|^2}{N_1 + N_2}}{m_1^{3/2} H_\tau^E(c_{12}) + m_2^{3/2} H_{\tau'}^E(c_{21})} \left[\frac{m_1^{3/2} H_\tau^E(c_{12})}{n_1} - \frac{m_2^{3/2} H_{\tau'}^E(c_{21})}{n_2} \right] \right).
\end{aligned}$$

This can be written as

$$\begin{aligned}
& \partial_t \left(\left(\frac{E_1}{n_1} - \frac{1}{2} \frac{|P_1|^2}{n_1 N_1} \right) - \left(\frac{E_2}{n_2} - \frac{1}{2} \frac{|P_2|^2}{n_2 N_2} \right) \right) \\
&= \tilde{\nu} - \left(\left(\frac{E_1}{n_1} - \frac{1}{2} \frac{|P_1|^2}{n_1 N_1} \right) - \left(\frac{E_2}{n_2} - \frac{1}{2} \frac{|P_2|^2}{n_2 N_2} \right) \right) + \frac{1}{2} \frac{m_2 (n_2 N_2 - n_1 N_1)}{(N_1 + N_2)^2} \frac{|P_1|^2}{n_1 N_1} + \frac{1}{2} \frac{m_1 (n_2 N_2 - n_1 N_1)}{(N_1 + N_2)^2} \frac{|P_2|^2}{n_2 N_2} \\
&+ P_1 \cdot P_2 \frac{n_1 N_1 - n_2 N_2}{(N_1 + N_2)^2 n_1 n_2} + \frac{(E_1 + E_2) - \frac{1}{2} \frac{|P_1 + P_2|^2}{N_1 + N_2}}{m_1^{3/2} H_\tau^E(c_{12}) + m_2^{3/2} H_{\tau'}^E(c_{21})} \left[\frac{m_1^{3/2} H_\tau^E(c_{12})}{n_1} - \frac{m_2^{3/2} H_{\tau'}^E(c_{21})}{n_2} \right] \\
&= \tilde{\nu} - \left(\left(\frac{E_1}{n_1} - \frac{|P_1|^2}{n_1 N_1} \right) - \left(\frac{E_2}{n_2} - \frac{|P_2|^2}{n_2 N_2} \right) \right) + \frac{1}{2} m_1 m_2 \frac{n_2 N_2 - n_1 N_1}{(N_1 + N_2)^2} \left| \frac{P_1}{N_1} - \frac{P_2}{N_2} \right|^2 \\
&+ \frac{(E_1 + E_2) - \frac{1}{2} \frac{|P_1 + P_2|^2}{N_1 + N_2}}{m_1^{3/2} H_\tau^E(c_{12}) + m_2^{3/2} H_{\tau'}^E(c_{21})} \left[\frac{m_1^{3/2} H_\tau^E(c_{12})}{n_1} - \frac{m_2^{3/2} H_{\tau'}^E(c_{21})}{n_2} \right].
\end{aligned}$$

Now, Duhamels formula gives

$$\begin{aligned}
& \left(\frac{E_1}{N_1} - \frac{1}{2} \frac{|P_1|^2}{m_1 N_1^2} \right) - \left(\frac{E_2}{N_2} - \frac{1}{2} \frac{|P_2|^2}{n_2 N_2} \right) \\
&= e^{-\tilde{\nu} t} \left(\left(\frac{E_1(0)}{n_1} - \frac{1}{2} \frac{|P_1(0)|^2}{n_1 N_1} \right) - \left(\frac{E_2(0)}{n_2} - \frac{1}{2} \frac{|P_2(0)|^2}{n_2 N_2} \right) \right) + \frac{1}{2} m_1 m_2 \frac{n_2 N_2 - n_1 N_1}{(N_1 + N_2)^2} e^{-\tilde{\nu} t} \int_0^t e^{\tilde{\nu} s} \left| \frac{P_2(s)}{N_2} - \frac{P_1(s)}{N_1} \right|^2 ds \\
&+ \left(E_1(0) + E_2(0) - \frac{1}{2} \frac{|P_1(0) + P_2(0)|^2}{N_1 + N_2} \right) e^{-\tilde{\nu} t} \int_0^t e^{\tilde{\nu} s} \left[\frac{\frac{m_1^{3/2} H_\tau^E(c_{12}(s))}{n_1} - \frac{m_2^{3/2} H_{\tau'}^E(c_{21}(s))}{n_2}}{m_1^{3/2} H_\tau^E(c_{12}) + m_2^{3/2} H_{\tau'}^E(c_{21})} \right] ds \\
&= e^{-\tilde{\nu} t} \left(\left(\frac{E_1(0)}{n_1} - \frac{1}{2} \frac{|P_1(0)|^2}{n_1 N_1} \right) - \left(\frac{E_2(0)}{n_2} - \frac{1}{2} \frac{|P_2(0)|^2}{n_2 N_2} \right) \right) + \frac{1}{2} m_1 m_2 \frac{n_2 N_2 - n_1 N_1}{(N_1 + N_2)^2} e^{-\tilde{\nu} t} \int_0^t e^{\tilde{\nu} s} e^{-2\tilde{\nu} s} \left| \frac{P_2(0)}{N_2} - \frac{P_1(0)}{N_1} \right|^2 ds \\
&+ \left(E_1(0) + E_2(0) - \frac{1}{2} \frac{|P_1(0) + P_2(0)|^2}{N_1 + N_2} \right) e^{-\tilde{\nu} t} \int_0^t e^{\tilde{\nu} s} \left[\frac{\frac{m_1^{3/2} H_\tau^E(c_{12}(s))}{n_1} - \frac{m_2^{3/2} H_{\tau'}^E(c_{21}(s))}{n_2}}{m_1^{3/2} H_\tau^E(c_{12}(s)) + m_2^{3/2} H_{\tau'}^E(c_{21}(s))} \right] ds \\
&= e^{-\tilde{\nu} t} \left(\left(\frac{E_1(0)}{n_1} - \frac{1}{2} \frac{|P_1(0)|^2}{n_1 N_1} \right) - \left(\frac{E_2(0)}{n_2} - \frac{1}{2} \frac{|P_2(0)|^2}{n_2 N_2} \right) \right) + \frac{1}{2} m_1 m_2 \frac{n_2 N_2 - n_1 N_1}{(N_1 + N_2)^2} e^{-\tilde{\nu} t} (1 - e^{-\tilde{\nu} t}) \left| \frac{P_2(0)}{N_2} - \frac{P_1(0)}{N_1} \right|^2 \\
&+ \left(E_1(0) + E_2(0) - \frac{1}{2} \frac{|P_1(0) + P_2(0)|^2}{N_1 + N_2} \right) e^{-\tilde{\nu} t} \int_0^t e^{\tilde{\nu} s} \left[\frac{\frac{m_1^{3/2} H_\tau^E(c_{12}(s))}{n_1} - \frac{m_2^{3/2} H_{\tau'}^E(c_{21}(s))}{n_2}}{m_1^{3/2} H_\tau^E(c_{12}(s)) + m_2^{3/2} H_{\tau'}^E(c_{21}(s))} \right] ds.
\end{aligned}$$

We get the last but one equality by using theorem 3.3.1 and the last equality by computing the integral. \square

Remark 5. In the classical case we get, as in remark 3, the relationship

$$\frac{n_1}{n_2} = \frac{m_1^{3/2} e^{-c_{12}}}{m_2^{3/2} e^{-c_{21}}}.$$

If we then compute the bracket

$$\left[\frac{\frac{m_1^{3/2} H_\tau^E(c_{12}(s))}{n_1} - \frac{m_2^{3/2} H_{\tau'}^E(c_{21}(s))}{n_2}}{m_1^{3/2} H_\tau^E(c_{12}) + m_2^{3/2} H_{\tau'}^E(c_{21})} \right]$$

for $\tau = \tau' = 0$, we obtain by an explicit computation of H_τ^E

$$\frac{\frac{m_1^{3/2}}{n_1} \frac{3}{2} e^{-c_{12}} \pi^{3/2} - \frac{m_2^{3/2}}{n_2} \frac{3}{2} e^{-c_{21}} \pi^{3/2}}{m_1^{3/2} \frac{3}{2} e^{-c_{12}} \pi^{3/2} + m_2^{3/2} \frac{3}{2} e^{-c_{21}} \pi^{3/2}} = \frac{\frac{m_1^{3/2}}{n_1} e^{-c_{12}} - \frac{m_2^{3/2}}{n_2} e^{-c_{21}}}{m_1^{3/2} e^{-c_{12}} + m_2^{3/2} e^{-c_{21}}} = 0$$

So in the classical-classical case, the last term of (21) vanishes, and we obtain the temperature convergence rate

$$\begin{aligned} & \left(\frac{E_1}{n_1} - \frac{1}{2} \frac{|P_1|^2}{n_1 N_1} \right) - \left(\frac{E_2}{n_2} - \frac{1}{2} \frac{|P_2|^2}{n_2 N_2} \right) \\ &= e^{-\bar{\nu}t} \left(\left(\frac{E_1(0)}{n_1} - \frac{1}{2} \frac{|P_1(0)|^2}{n_1 N_1} \right) - \left(\frac{E_2(0)}{n_2} - \frac{1}{2} \frac{|P_2(0)|^2}{n_2 N_2} \right) \right) + \frac{1}{2} m_1 m_2 \frac{n_2 N_2 - n_1 N_1}{(N_1 + N_2)^2} e^{-\bar{\nu}t} (1 - e^{-\bar{\nu}t}) \left| \frac{P_2(0)}{N_2} - \frac{P_1(0)}{N_1} \right|^2. \end{aligned}$$

4 Motivation of the structure of the local equilibria

In this section, we motivate the form of the local equilibria in (1) This will motivate later the choice of our numerical scheme. For this, it will be convenient to define the following notations. We denote

$$\begin{aligned} \mathcal{K}_{11} &= (e^{-\alpha_{11} \cdot \mathbf{p}_1} + \tau)^{-1}, & \mathcal{K}_{22} &= (e^{-\alpha_{22} \cdot \mathbf{p}_2} + \tau')^{-1}, \\ \mathcal{K}_{12} &= (e^{-\alpha_{12} \cdot \mathbf{p}_1} + \tau)^{-1}, & \mathcal{K}_{21} &= (e^{-\alpha_{21} \cdot \mathbf{p}_2} + \tau')^{-1} \end{aligned} \quad (24)$$

where

$$\mathbf{p}_k(p) := \left(1, p, \frac{|p|^2}{2m_k} \right)^\top, \quad k = 1, 2 \quad (25)$$

and the parameters $(a_1, a_2, b_1, b_2, b, c_1, c_2, c_{12}, c_{21})$ can be mapped one-to-one to $\alpha_{kj} = (\alpha_{kj}^0, \alpha_{kj}^1, \alpha_{kj}^2)$, $k, j = 1, 2$. Further, we recall the function h_τ defined by (11) is convex, therefore it follows

$$h_\tau(z) \geq h_\tau(y) + \ln(y)(z - y), \quad (26)$$

for all $y, z > 0$ if $\tau = 0, -1$ and $0 < y, z < 1$ if $\tau = +1$.

4.1 The one species local equilibria

We seek a solution of the entropy minimization problem

$$\min_{g \in \chi_k} \int h_\tau(g) dv, \quad k \in \{1, 2\}, \quad (27)$$

where

$$\chi_k = \left\{ g \mid g \geq 0, (1 + |p|^2)g \in L^1(\mathbb{R}^3), \int \mathbf{p}_k(p)(g - f_k) dp = 0 \right\}. \quad (28)$$

The choice of the set χ_k ensures the conservation properties (4) for intra-species collisions. Indeed, by standard optimization theory, any critical point $(\mathcal{K}_{kk}, \lambda^{kk})$ of the Lagrange functional $L_k: \chi_k \times \mathbb{R}^5 \rightarrow \mathbb{R}$, given by

$$L_k(g, \alpha) = \int h(g)dp - \alpha \cdot \int \mathbf{p}_k(p)(g - f_k)dp, \quad (29)$$

satisfies the first-order optimality condition

$$\frac{\delta L_k}{\delta g}(\mathcal{K}_{kk}, \lambda^{kk}) = \left(\ln \frac{\mathcal{K}_{kk}}{1 - \tau_k \mathcal{K}_{kk}} - \lambda^{kk} \cdot \mathbf{p}_k(p) \right) = 0, \quad (30)$$

with $\tau_1 = \tau$ and $\tau_2 = \tau'$. This implies then that

$$\mathcal{K}_{kk} = (\exp(\lambda^{kk} \cdot \mathbf{p}_k(p)) + \tau_k)^{-1}. \quad (31)$$

Theorem 3.1.1 shows in a rigorous way that there exists a unique function of the form (31) that satisfies these constraints. Therefore, we can prove the following theorem.

Theorem 4.1.1. *The local equilibrium \mathcal{K}_{kk} is the unique minimizer of (27).*

Proof. According to (26)

$$h_{\tau_k}(g) \geq h_{\tau_k}(\mathcal{K}_{kk}) + \lambda^{kk} \cdot \mathbf{p}_k(g - \mathcal{K}_{kk}), \quad (32)$$

point-wise in p . Thus it follows that for all $g \in \chi_k$,

$$\int h_{\tau_k}(g)dp \geq \int h_{\tau_k}(\mathcal{K}_{kk})dp + \int \lambda^{kk} \cdot \mathbf{p}_k(g - \mathcal{K}_{kk})dp = \int h_{\tau_k}(\mathcal{K}_{kk})dp \quad (33)$$

Hence \mathcal{K}_{kk} is a minimizer of (27), and uniqueness follows directly from the strict convexity of h_{τ_k} . \square

4.2 The mixture local equilibria

For interactions between species, we seek a solution of the entropy minimization problem

$$\min_{g_1, g_2 \in \chi_{12}} \int h_{\tau}(g_1)dp + \int h_{\tau'}(g_2)dp, \quad (34)$$

where

$$\chi_{12} = \left\{ (g_1, g_2) \mid g_1, g_2 > 0, (1 + |p|^2)g_1, (1 + |p|^2)g_2 \in L^1(\mathbb{R}^3), \right. \\ \left. \int g_1 dp = \int f_1 dp, \quad \int g_2 dp = \int f_2 dp, \right. \\ \left. \int \left(\frac{p}{2m_1} \right) (g_1 - f_1) dp + \int \left(\frac{p}{2m_2} \right) (g_2 - f_2) dp = 0 \right\}. \quad (35)$$

Here, χ_{12} is chosen such that the constraints (5) for inter-species collisions are satisfied. Similar to the case of intra-species collisions, we consider the Lagrange functional $L: \chi \times \mathbb{R} \times \mathbb{R} \times \mathbb{R}^3 \times \mathbb{R} \rightarrow \mathbb{R}$

$$\begin{aligned}
L(g_1, g_2, \alpha_0^1, \alpha_0^2, \alpha_1, \alpha_2) &= \int h(g_1)dp + \int h(g_2)dp \\
&\quad - \alpha_0^1 \int (g_1 - f_1)dp - \alpha_0^2 \int (g_2 - f_2)dp \\
&\quad - \alpha_1 \cdot \left(\int p(g_1 - f_1)dp + \int p(g_2 - f_2)dp \right) \\
&\quad - \alpha_2 \cdot \left(\int \frac{|p|^2}{2m_1}(g_1 - f_1)dp + \int \frac{|p|^2}{2m_2}(g_2 - f_2)dp \right).
\end{aligned} \tag{36}$$

Any critical point $(\mathcal{K}_{12}, \mathcal{K}_{21}, \lambda_0^1, \lambda_0^2, \lambda_1, \lambda_2)$ of L satisfies the first-order optimality conditions

$$\frac{\delta L}{\delta g_1}(\mathcal{K}_{12}, \mathcal{K}_{21}, \lambda_0^1, \lambda_0^2, \lambda_1, \lambda_2) = \ln \frac{\mathcal{K}_{12}}{1 - \tau \mathcal{K}_{12}} - \lambda^{12} \cdot \mathbf{p}_1(p) = 0, \tag{37}$$

$$\frac{\delta L}{\delta g_2}(\mathcal{K}_{12}, \mathcal{K}_{21}, \lambda_0^1, \lambda_0^2, \lambda_1, \lambda_2) = \ln \frac{\mathcal{K}_{21}}{1 - \tau \mathcal{K}_{21}} - \lambda^{21} \cdot \mathbf{p}_2(p) = 0, \tag{38}$$

where $\lambda^{12} = (\lambda_0^1, \lambda_1, \lambda_2)$ and $\lambda^{21} = (\lambda_0^2, \lambda_1, \lambda_2)$. Therefore

$$\mathcal{K}_{12} = (\exp(\lambda^{12} \cdot \mathbf{p}_1(p)) + \tau)^{-1}, \tag{39}$$

$$\mathcal{K}_{21} = (\exp(\lambda^{21} \cdot \mathbf{p}_2(p)) + \tau)^{-1}. \tag{40}$$

Since we only require conservation of the combined momentum and kinetic energy, there is only one Lagrange multiplier for the momentum constraint and one Lagrange multiplier for the energy constraint. Hence, $\lambda_1^{12} = \lambda_1^{21}$ and $\lambda_2^{12} = \lambda_2^{21}$ in (40). When we are in the classical case ($\tau = 0$), this restriction is the same as the one used in [21], but more restrictive than the model in [28].

Theorem 3.1.2 shows the existence of functions of the form (40) which satisfy the constraints in (4) and (5). As in the single species case, it follows that these functions are unique minimizer of the corresponding minimization problem.

Theorem 4.2.1. $(\mathcal{K}_{12}, \mathcal{K}_{21})$ as defined in (40) is the unique minimizer of (34).

Proof. According to (26)

$$h_\tau(g) \geq h_{\tau_k}(\mathcal{K}_{kj}) + \lambda^{kj} \cdot \mathbf{p}_k(g - \mathcal{K}_{kj}), \tag{41}$$

point-wise in p , for any measurable function g and $k, j \in \{1, 2\}$. Therefore it follows that for any measurable functions g_1 and g_2 ,

$$\begin{aligned}
\int h_\tau(g_1)dp + \int h_{\tau'}(g_2)dp &\geq \int h_\tau(\mathcal{K}_{12})dp + \int h_{\tau'}(\mathcal{K}_{21})dp \\
&\quad + \lambda^{12} \cdot \int \mathbf{p}_1(g_1 - \mathcal{K}_{12})dp + \lambda^{21} \cdot \int \mathbf{p}_2(g_2 - \mathcal{K}_{21})dp.
\end{aligned} \tag{42}$$

Since $\lambda_1^{12} = \lambda_1^{21}$ and $\lambda_2^{12} = \lambda_2^{21}$,

$$\begin{aligned}
\lambda^{12} \cdot \int \mathbf{p}_1(g_1 - \mathcal{K}_{12})dp + \lambda^{21} \cdot \int \mathbf{p}_2(g_2 - \mathcal{K}_{21})dp &= \lambda_0^{12} \int (g_1 - \mathcal{K}_{12})dp + \lambda_0^{21} \int (g_2 - \mathcal{K}_{21})dp \\
&\quad + \lambda_1^{12} \cdot \left(\int p(g_1 - \mathcal{K}_{12})dp + \int p(g_2 - \mathcal{K}_{21})dp \right) + \lambda_2^{12} \cdot \left(\int \frac{|p|^2}{2m_1}(g_1 - \mathcal{K}_{12})dp + \int \frac{|p|^2}{2m_2}(g_2 - \mathcal{K}_{21})dp \right).
\end{aligned} \tag{43}$$

If (g_1, g_2) and $(\mathcal{K}_{12}, \mathcal{K}_{21})$ are elements of χ_{12} , then the constraints in (35) imply that each of the terms above is zero. In such cases, (42) reduces to

$$\int h_\tau(g_1)dp + \int h_{\tau'}(g_2)dp \geq \int h_\tau(\mathcal{K}_{12})dp + \int h_{\tau'}(\mathcal{K}_{21})dp, \quad (44)$$

which shows that $(\mathcal{K}_{12}, \mathcal{K}_{21})$ solves (34). Since h_{τ_k} is strictly convex, it follows that this solution is unique. \square

5 Numerical scheme

5.1 Time discretization

Let $k, j = 1, 2$ and $k \neq j$. We write (1) as

$$\partial_t f_k + \mathcal{T}_k(f_k) = \mathcal{R}_k(f_k, f_j) \quad (45)$$

with the combined relaxation operator

$$\mathcal{R}_k(f_k, f_j) = \mathcal{R}_{kk} + \mathcal{R}_{kj} = \nu_{kk} n_k (\mathcal{K}_{kk} - f_k) + \nu_{kj} n_j (\mathcal{K}_{kj} - f_k) \quad (46)$$

and the transport operator

$$\mathcal{T}_k(f_k) = \frac{p}{m_k} \cdot \nabla_x f_k. \quad (47)$$

In the following, for simplicity, we assume that the collision frequencies $\tilde{\nu}_{kk} := \nu_{kk} n_k$ and $\tilde{\nu}_{kj} := \nu_{kj} n_k$ are constant in x and t . But an extension to an x and t dependence of the collision frequency would also be possible. Large collision frequencies result in a stiff relaxation operator such that an implicit time discretization for the relaxation part is a convenient choice. So we pursue implicit-explicit (IMEX) schemes where \mathcal{R}_k is treated implicitly and \mathcal{T}_i is treated explicitly.

Given $t_\ell = \ell \Delta t$ for $\ell \in \mathbb{N}_0$, a simple update of $f_k^\ell \approx f_k(x, p, t_\ell)$ from t_ℓ to $t_{\ell+1}$ uses the approximation

$$\mathcal{R}_k(f_k^{\ell+1}, f_j^{\ell+1}) \approx \tilde{\nu}_{kk} (\mathcal{K}_{kk}^{\ell+1} - f_k^{\ell+1}) + \tilde{\nu}_{kj} (\mathcal{K}_{kj}^{\ell+1} - f_k^{\ell+1}), \quad (48)$$

where $\mathcal{K}_{kk}^{\ell+1}$ and $\mathcal{K}_{kj}^{\ell+1}$ are discrete target functions that, as described in Section 5.1.3, depend on $f_k^{\ell+1}$ and $f_j^{\ell+1}$ via the solution of a convex minimization problem that is inspired by the work in [23]. By this procedure, \mathcal{K}_{kk} and \mathcal{K}_{kj} are evaluated exactly at the next time step (up to numerical tolerances) which results in the preservation of conservation properties, and the first-order version inherits additional properties from the continuum model.

5.1.1 First-order splitting

We split the relaxation and transport operators in (1).

Relaxation. We perform the relaxation step in each spatial cell by a backward Euler method

$$\frac{f_k^* - f_k^\ell}{\Delta t} = \mathcal{R}_k(f_k^*, f_j^*), \quad (49)$$

which can be rewritten into the convex combination

$$f_k^* = d_k f_k^\ell + d_k \Delta t (\tilde{\nu}_{kk} \mathcal{K}_{kk}^* + \tilde{\nu}_{kj} \mathcal{K}_{kj}^*) \quad (50)$$

with

$$d_k = \frac{1}{1 + \Delta t (\tilde{\nu}_{kk} + \tilde{\nu}_{kj})}. \quad (51)$$

The equation (50) represents an explicit update formula for f_k^* provided that \mathcal{K}_{kk}^* and \mathcal{K}_{kj}^* can be expressed as functions of f_k^ℓ . In Section 5.1.3 we show how to determine \mathcal{K}_{kk}^* and \mathcal{K}_{kj}^* in a structure-preserving way.

Transport. We compute the transport in x for $f_k^{\ell+1}$ by a forward Euler method with initial data f_k^* :

$$\frac{f_k^{\ell+1} - f_k^*}{\Delta t} + \mathcal{T}_k(f_k^*) = 0. \quad (52)$$

Details on the numerical approximation of \mathcal{T}_k are presented in section 5.2.

5.1.2 Second-order IMEX Runge-Kutta

We use the following Butcher tableaux [2] for a second-order approach

$$\begin{array}{c|ccc} 0 & & & \\ \gamma & 0 & \gamma & \\ \hline 1 & 0 & 1-\gamma & \gamma \\ \hline & 0 & 1-\gamma & \gamma \end{array} \quad \begin{array}{c|ccc} 0 & & & \\ \gamma & \gamma & & \\ \hline 1 & \delta & 1-\delta & 0 \\ \hline & \delta & 1-\delta & 0 \end{array} \quad (53)$$

with

$$\gamma = 1 - \frac{\sqrt{2}}{2} \quad \text{and} \quad \delta = 1 - \frac{1}{2\gamma}. \quad (54)$$

The left table applies to the relaxation part, and the right table applies to the transport terms. This IMEX Runge-Kutta scheme is L-stable and globally stiffly accurate.

Applying this method to (1) and using the constants

$$d_k = \frac{1}{1 + \gamma \Delta t (\tilde{\nu}_{kk} + \tilde{\nu}_{kj})}, \quad (55)$$

we can write the stages in the scheme as convex combination of three terms

$$f_k^{(1)} = d_k G_k^{(1)} + d_k \gamma \Delta t \tilde{\nu}_{kk} \mathcal{K}_{kk}^{(1)} + d_k \gamma \Delta t \tilde{\nu}_{kj} \mathcal{K}_{kj}^{(1)} \quad (56a)$$

$$f_k^{(2)} = d_k G_k^{(2)} + d_k \gamma \Delta t \tilde{\nu}_{kk} \mathcal{K}_{kk}^{(2)} + d_k \gamma \Delta t \tilde{\nu}_{kj} \mathcal{K}_{kj}^{(2)}, \quad (56b)$$

$$f_k^{\ell+1} = f_k^{(2)} \quad (56c)$$

where

$$G_k^{(1)} = f_k^\ell - \Delta t \gamma \mathcal{T}_k(f_k^\ell) \quad (57a)$$

$$G_k^{(2)} = f_k^\ell - \Delta t \delta \mathcal{T}_k(f_k^\ell) - \Delta t (1 - \delta) \mathcal{T}_k(f_k^{(1)}) + \Delta t (1 - \gamma) \mathcal{R}_k(f_k^{(1)}, f_j^{(1)}) \quad (57b)$$

depend on known data. For each stage, we have to determine the corresponding values of the target functions in order to update the distribution functions. In the following section, we explain how this can be done.

5.1.3 General implicit solver

We write the implicit updates in (50) and (56) in a generic steady state form

$$\psi_k = d_k G_k + d_k \gamma \Delta t (\tilde{\nu}_{kk} \mathcal{K}_{kk} + \tilde{\nu}_{kj} \mathcal{K}_{kj}). \quad (58)$$

The functions \mathcal{K}_{kk} and \mathcal{K}_{kj} are the unique target functions associated to ψ_k ,

$$d_k = \frac{1}{1 + \gamma \Delta t (\tilde{\nu}_{kk} + \tilde{\nu}_{kj})}, \quad (59)$$

and G_k is a known function. We want to express \mathcal{K}_{kk} and \mathcal{K}_{kj} as functions of G_k and G_j so that (58) is an explicit update formula for ψ_k . In Section 3, the existence and uniqueness of \mathcal{K}_{kk} and \mathcal{K}_{kj} are proven by algebraic considerations. In order to determine their values we follow a different approach inspired by section 4. Applying the conservation properties (4) and (5) to (58) leads to

$$\begin{aligned} & \int \tilde{\nu}_{11} \mathcal{K}_{11} \mathbf{p}_1 dp + \int \tilde{\nu}_{22} \mathcal{K}_{22} \mathbf{p}_2 dp + \int \tilde{\nu}_{12} \mathcal{K}_{12} \mathbf{p}_1 dp + \int \tilde{\nu}_{21} \mathcal{K}_{21} \mathbf{p}_2 dp \\ & \stackrel{(4),(5)}{=} \int \tilde{\nu}_{11} \psi_1 \mathbf{p}_1 dp + \int \tilde{\nu}_{22} \psi_2 \mathbf{p}_2 dp + \int \tilde{\nu}_{12} \psi_1 \mathbf{p}_1 dp + \int \tilde{\nu}_{21} \psi_2 \mathbf{p}_2 dp \\ & \stackrel{(58)}{=} \int \tilde{\nu}_{11} d_1 [G_1 + \Delta t \gamma \tilde{\nu}_{11} \mathcal{K}_{11} + \Delta t \gamma \tilde{\nu}_{12} \mathcal{K}_{12}] \mathbf{p}_1 dp + \int \tilde{\nu}_{22} d_2 [G_2 + \Delta t \gamma \tilde{\nu}_{22} \mathcal{K}_{22} + \Delta t \gamma \tilde{\nu}_{21} \mathcal{K}_{21}] \mathbf{p}_2 dp \\ & \quad + \int \tilde{\nu}_{12} d_1 [G_1 + \Delta t \gamma \tilde{\nu}_{11} \mathcal{K}_{11} + \Delta t \gamma \tilde{\nu}_{12} \mathcal{K}_{12}] \mathbf{p}_1 dp + \int \tilde{\nu}_{21} d_2 [G_2 + \Delta t \gamma \tilde{\nu}_{22} \mathcal{K}_{22} + \Delta t \gamma \tilde{\nu}_{21} \mathcal{K}_{21}] \mathbf{p}_2 dp \end{aligned} \quad (60)$$

Sorting terms yields the following moment equations

$$\begin{aligned} & \int d_1 (\tilde{\nu}_{11} \mathcal{K}_{11} + \tilde{\nu}_{12} \mathcal{K}_{12}) \mathbf{p}_1 dp + \int d_2 (\tilde{\nu}_{21} \mathcal{K}_{21} + \tilde{\nu}_{22} \mathcal{K}_{22}) \mathbf{p}_2 dp \\ & = \int d_1 (\tilde{\nu}_{11} + \tilde{\nu}_{12}) G_1 \mathbf{p}_1 + \int d_2 (\tilde{\nu}_{21} + \tilde{\nu}_{22}) G_2 \mathbf{p}_2 dp \end{aligned} \quad (61)$$

which provide a set of constraints to determine \mathcal{K}_{kk} and \mathcal{K}_{kj} from the given data G_k and G_j . These represent first-order optimality conditions associated to the minimization of the convex potential function

$$\begin{aligned} \varphi_{\text{tot}}(\alpha_1, \alpha_2, \alpha) = & \int [d_1 \tilde{\nu}_{11} w(\mathcal{K}_{11}) + d_2 \tilde{\nu}_{22} w(\mathcal{K}_{22}) + d_1 \tilde{\nu}_{12} w(\mathcal{K}_{12}) + d_2 \tilde{\nu}_{21} w(\mathcal{K}_{21})] dp \\ & - \mu_1 \cdot \alpha_1 - \mu_2 \cdot \alpha_2 - \mu \cdot \alpha \end{aligned} \quad (62)$$

where $\alpha_k = (\alpha_k^0, \alpha_k^1, \alpha_k^2)$ and $\alpha = (\alpha_{12}^0, \alpha_{21}^0, \alpha^1, \alpha^2)^\top$; the auxiliary function reads

$$w(\mathcal{K}_{kj, \tau}) = \begin{cases} \mathcal{K}_{kj, 0} & \text{for } \tau_k = 0, \\ \log(1 - \tau_k \mathcal{K}_{kj, \tau_k}) & \text{else;} \end{cases} \quad (63)$$

the given moments are

$$\mu_k = \begin{pmatrix} \mu_k^0 \\ \mu_k^1 \\ \mu_k^2 \end{pmatrix} = \int d_k \tilde{\nu}_{kk} G_k \mathbf{p}_k dp \quad (64)$$

for $k = 1, 2$; and

$$\mu = \begin{pmatrix} \mu_{12}^0 \\ \mu_{21}^0 \\ \mu^1 \\ \mu^2 \end{pmatrix} = \int \left[\begin{pmatrix} 1 \\ 0 \\ p \\ \frac{|p|^2}{2m_1} \end{pmatrix} d_1 \tilde{\nu}_{12} G_1 + \begin{pmatrix} 0 \\ 1 \\ p \\ \frac{|p|^2}{2m_2} \end{pmatrix} d_2 \tilde{\nu}_{21} G_2 \right] dp. \quad (65)$$

The minimization problem can be decoupled as follows:

Proposition 5.1. *The components of the minimizer of (62) can be found by minimizing the following three convex potential functions independently:*

$$\varphi_k(\alpha_k) = \int d_k \tilde{\nu}_{kk} w(\mathcal{K}_{kk}) dp + \mu_k \cdot \alpha_k \quad \text{for } k = 1, 2 \quad \text{and} \quad (66)$$

$$\varphi(\alpha) = \int [d_1 \tilde{\nu}_{12} w(\mathcal{K}_{12}) + d_2 \tilde{\nu}_{21} w(\mathcal{K}_{21})] dp + \mu \cdot \alpha \quad (67)$$

and the minimum of (62) is the sum of their minima.

Proof. The statement is trivial because $\varphi_{\text{tot}}(\alpha_1, \alpha_2, \alpha) = \varphi_1(\alpha_1) + \varphi_2(\alpha_2) + \varphi_1(\alpha)$. \square

The minimum of each potential function in (66) and (67) is found using Newton's method for convex optimization. More details are given in Section 5.4.

Actually, we can link these potential functions to dual problems when we reformulate the modelling problem by using Lagrange functionals. For intra-species interactions, the Lagrange functional reads

$$L_k(g, \lambda) = \int h_{\tau_k}(g) dp - \lambda \cdot \int \mathbf{p}_k (g - f_k) dp \quad (68)$$

using $h_{\tau_k}(g)$ given by (11). The first integral in (68) is the entropy functional; the other integrals describe the conservation properties as constraints. The Lagrange multipliers λ solve the dual problem

$$\alpha_k = \operatorname{argmin}_{\lambda \in \Lambda_k} \int w(\mathcal{K}_{kk}(\lambda)) dp + \lambda \cdot \int \mathbf{p}_k f_k dp \quad (69)$$

where $\Lambda_k = \{\lambda \in \mathbb{R}^5 \mid \int \mathcal{K}_{kk}(\lambda)(1 + |p|^2) dp < \infty\}$. Analogously, we can formulate the dual problem for inter-species interactions:

$$\begin{aligned} (\alpha_{12}, \alpha_{21}) = \operatorname{argmin}_{(\lambda_{12}, \lambda_{21}) \in \Lambda} & \left\{ \int w(\mathcal{K}_{12}(\lambda)) + w(\mathcal{K}_{21}(\lambda)) dp + \lambda_{12}^0 \int f_1 dp + \lambda_{21}^0 \int f_2 dp \right. \\ & \left. + \lambda^1 \cdot \int p(f_1 + f_2) dp + \lambda^2 \int |p|^2 \left(\frac{1}{2m_1} f_1 + \frac{1}{2m_2} f_2 \right) dp \right\} \end{aligned} \quad (70)$$

for $\alpha_{kj} = (\alpha_{kj}^0, \alpha^1, \alpha^2)$ and where $\Lambda = \{(\lambda_{12}, \lambda_{21}) \in \mathbb{R}^5 \mid \int \mathcal{K}_{kj}(\lambda_{kj})(1 + |p|^2) dp < \infty \text{ for } k, j = 1, 2; k \neq j\}$. We recognize the close relationship of (66) with (69), respective of (67) with (70). The dual problems have unique solutions according to Section 4. This is inherited to the potential functions because $d_k \tilde{\nu}_{kj}$ is independent of p .

5.2 Space discretization

We assume a slab geometry, i.e. $\partial_{x^2} f_k = \partial_{x^3} f_k = 0$. So we reduce the physical space dimension to one dimension and set $x := x^1$ while the momentum domain remains three dimensional ($p = (p^1, p^2, p^3)$). We divide the spatial domain $[x_{\min}, x_{\max}]$ into uniform cells $I_i = [x_i - \frac{\Delta x}{2}, x_i + \frac{\Delta x}{2}]$ for $i \in \{0, \dots, I\}$.

We employ a second-order finite volume framework using approximate cell-averaged quantities

$$f_{k,i}^\ell \approx \frac{1}{\Delta x} \int_{I_i} f_k(x, p, t^\ell) dx. \quad (71)$$

The relaxation operators are approximated to second order by

$$\mathcal{R}_{k,i}^\ell = \mathcal{R}_k(f_{k,i}^\ell, f_{j,i}^\ell) \approx \frac{1}{\Delta x} \int_{I_i} \mathcal{R}(f_k(x, p, t^\ell), f_j(x, p, t^\ell)) dx. \quad (72)$$

Whereas the transport operator \mathcal{T}_k is discretized with numerical fluxes $\mathcal{F}_{i+\frac{1}{2}}$ by

$$\mathcal{T}_k(g) \approx \mathcal{T}_{i,k}(g) = \frac{1}{\Delta x} \left(\mathcal{F}_{k+\frac{1}{2}}(g) - \mathcal{F}_{i-\frac{1}{2}}(g) \right) \quad (73)$$

for any grid function $g = \{g_i\}$. We follow [33] and use

$$\mathcal{F}_{i+\frac{1}{2}}(g) = \frac{p^1}{2m} (g_{i+1} + g_i) - \frac{|p^1|}{2m} \left(g_{i+1} - g_i - \phi_{i+\frac{1}{2}}(g) \right) \quad (74)$$

where $\phi_{i+\frac{1}{2}}$ is a flux limiter. The choice $\phi_{i+\frac{1}{2}} = 0$ leads to a first-order approximation, and a second-order method is provided by

$$\phi_{i+\frac{1}{2}}(g) = \text{minmod}((g_i - g_{i-1}), (g_{i+1} - g_i), (g_{i+2} - g_{i+1})) \quad (75)$$

where

$$\text{minmod}(a, b, c) = \begin{cases} s \min(|a|, |b|, |c|), & \text{sign}(a) = \text{sign}(b) = \text{sign}(c) =: s, \\ 0, & \text{otherwise.} \end{cases} \quad (76)$$

We guarantee positivity during a simple forward Euler update of (52) by enforcing the CFL condition

$$\Delta t < \alpha \frac{m \Delta x}{\max |p^1|} \quad (77)$$

with $\alpha = 1$ for the first-order flux and $\alpha = \frac{2}{3}$ for the second-order flux. (See Proposition 5.2.)

5.3 Properties of the semi-discrete scheme

In this section, we review the positivity preservation, conservation properties, and the entropy behavior of the semi-discrete scheme.

5.3.1 Positivity of distribution functions

The first-order time stepping scheme in Section 5.1.1 preserves positivity for both first- and second-order numerical fluxes in space; see Proposition 5.2. We discuss the positivity for the second-order scheme 5.1.2 in Proposition 5.3, and give a sufficient criterion for the space homogeneous case. Additionally, we show that the upper bound for distribution functions of fermions is preserved by our scheme; see Proposition 5.4.

Proposition 5.2. *The first-order time discretization in Section 5.1.1 together with the space discretization described in Section 5.2 is positivity preserving, provided that*

$$\Delta t \leq \beta \frac{m_k \Delta x}{\max |p^1|}, \quad (78)$$

with $\beta = 1$ and $\beta = \frac{2}{3}$ for the first-order and second-order fluxes, respectively.

Proof. The proof can be performed analogously to the proof of proposition 5.1 in [23]. \square

Second-order time-stepping makes it more difficult to guarantee positivity. Nevertheless, we derive some sufficient conditions on Δt in order to preserve positivity in the second-order scheme presented in Section 5.1.2.

Proposition 5.3. *For the space homogeneous case, the second-order IMEX scheme presented in Section 5.1.2 is positivity preserving provided that*

$$\Delta t \leq \frac{1}{(1 - 2\gamma)(\tilde{\nu}_{kk} + \tilde{\nu}_{kj})} \quad (79)$$

for $k, j = 1, 2$.

Proof. The proof can be performed analogously to the proof of proposition 5.2 in [23]. \square

For large collision frequencies ν_{kj} , the time step condition (79) can be restrictive. So one might be interested in enforcing the milder (but still sufficient) local condition

$$\Delta t \leq \frac{f_k^\ell}{(1 - \gamma) \left[(\tilde{\nu}_{kk} + \tilde{\nu}_{kj}) f_k^{(1)} - (\tilde{\nu}_{kk} A_{kk}^{(1)} + \tilde{\nu}_{kj} A_{kj}^{(1)}) \right]}. \quad (80)$$

Large collision frequencies push the numerical kinetic distribution to the corresponding target function. Hence, the denominator in (80) becomes large, and the condition is not restrictive.

A distribution function of a fermion has the additional upper bound $f < 1$. Our scheme preserves this property which is shown in the following propositions.

Proposition 5.4. *If f_k represents the distribution function of a fermion with $f_k^\ell < 1$, the time discretization in Section 5.1.1 together with the space discretization described in Section 5.2 leads to $f_k^{\ell+1} < 1$.*

Proof. Let $f_k^\ell < 1$. The local equilibrium of a fermion is a Fermi-Dirac distribution function \mathcal{F} for which $0 < \mathcal{F} < 1$ by definition. Hence, for the relaxation step it holds

$$f_k^* = d_k f_k^\ell + d_k \Delta t (\tilde{\nu}_{kk} \mathcal{F}_{kk}^* + \tilde{\nu}_{kj} \mathcal{F}_{kj}^*) < d_k + d_k \Delta t (\tilde{\nu}_{kk} + \tilde{\nu}_{kj}) = 1. \quad (81)$$

Here, we used the definition of d_k given by (55). For the transport step (52), the first-order fluxes lead to

$$f_{k,i}^{\ell+1} = \left(1 - \frac{\Delta t}{m_k \Delta x} |p^1|\right) f_{k,i}^* + \frac{\Delta t}{m_k \Delta x} |p^1| f_{k,i-\text{sign}(p^1)}^* \stackrel{(81)}{\leq} \left(1 - \frac{\Delta t}{m_k \Delta x} |p^1|\right) + \frac{\Delta t}{m_k \Delta x} |p^1| = 1.$$

For the second-order fluxes, define $\sigma := \text{sign}(f_{k,i}^* - f_{k,i-1}^*)$. We conclude that

$$\begin{aligned} \phi_{i+\frac{1}{2}}(f_k^*) &\leq \begin{cases} 0 & \text{if } \sigma = -1 \\ f_{k,i+1}^* - f_{k,i}^* & \text{if } \sigma = +1 \end{cases}, \\ -\phi_{i-\frac{1}{2}}(f_k^*) &\leq \begin{cases} f_{k,i-1}^* - f_{k,i}^* & \text{if } \sigma = -1 \\ 0 & \text{if } \sigma = +1 \end{cases}. \end{aligned}$$

It follows that

$$\begin{aligned} f_{k,i}^{\ell+1} &\stackrel{(52)}{=} \left(1 - \frac{\Delta t}{m_k \Delta x} |p^1|\right) f_{k,i}^* + \frac{\Delta t}{m_k \Delta x} |p^1| f_{k,i-\text{sign}(p^1)}^* + \frac{\Delta t}{m_k \Delta x} \frac{|p^1|}{2} (\phi_{i+\frac{1}{2}}(f_k^*) - \phi_{i-\frac{1}{2}}(f_k^*)) \\ &\leq \left(1 - \frac{\Delta t}{m_k \Delta x} |p^1|\right) f_{k,i}^* + \frac{\Delta t}{m_k \Delta x} |p^1| f_{k,i-\text{sign}(p^1)}^* + \frac{\Delta t}{m_k \Delta x} \frac{|p^1|}{2} \begin{cases} (f_{k,i-1}^* - f_{k,i}^*) & \text{if } \sigma = -1 \\ (f_{k,i+1}^* - f_{k,i}^*) & \text{if } \sigma = +1 \end{cases} \\ &= \left(1 - \frac{3}{2} \frac{\Delta t}{m_k \Delta x} |p^1|\right) f_{k,i}^* + \frac{\Delta t}{m_k \Delta x} |p^1| f_{k,i-\text{sign}(p^1)}^* + \frac{\Delta t}{m_k \Delta x} \frac{|p^1|}{2} \begin{cases} f_{k,i-1}^* & \text{if } \sigma = -1 \\ f_{k,i+1}^* & \text{if } \sigma = +1 \end{cases} \\ &\stackrel{(81)}{\leq} 1. \end{aligned}$$

□

Proposition 5.5. *If f_k represents the distribution function of a fermion with $f_k^\ell < 1$, the time discretization in Section 5.1.2 leads to $f_k^{\ell+1} < 1$ for the space homogeneous case.*

Proof. Let $f_k^\ell < 1$. The local equilibrium of a fermion is a Fermi-Dirac distribution function \mathcal{F} for which $0 < \mathcal{F} < 1$ by definition. Hence,

$$\begin{aligned} f_k^{\ell+1} &= d_k \left[f_k^\ell + \Delta t(1 - \gamma)(\tilde{\nu}_{kk} \mathcal{F}_{kk}^{(1)} + \tilde{\nu}_{kj} \mathcal{F}_{kj}^{(1)} - (\tilde{\nu}_{kk} + \tilde{\nu}_{kj}) f_k^{(1)}) \right] + \gamma \Delta t d_k (\tilde{\nu}_{kk} \mathcal{F}_{kk}^{(2)} + \tilde{\nu}_{kj} \mathcal{F}_{kj}^{(2)}) \\ &= d_k \left[f_k^\ell (1 - 2\Delta t(1 - \gamma)d_k) + \Delta t(1 - \gamma)d_k (\tilde{\nu}_{kk} \mathcal{F}_{kk}^{(1)} + \tilde{\nu}_{kj} \mathcal{F}_{kj}^{(1)}) \right] + \gamma \Delta t d_k (\tilde{\nu}_{kk} \mathcal{F}_{kk}^{(2)} + \tilde{\nu}_{kj} \mathcal{F}_{kj}^{(2)}) \\ &< d_k [1 - 2\Delta t(1 - \gamma)d_k + 2\Delta t(1 - \gamma)d_k + \gamma \Delta t(\tilde{\nu}_{kk} + \tilde{\nu}_{kj})] = 1. \end{aligned} \tag{82}$$

□

5.3.2 Conservation of mass, total momentum and total energy

In this section, we concern the conservation of mass, total momentum, and total energy for the semi-discrete scheme. The proofs of the following propositions work analogously as and can be found in the proofs of proposition 5.3 and 5.4 in [23].

Proposition 5.6. *The relaxation step in the first-order splitting scheme presented in Section 5.1.1 satisfies the conservation laws*

$$\int m_1 f_1^* dp = \int m_1 f_1^\ell dp, \quad \int m_2 f_2^* dp = \int m_2 f_2^\ell dp, \quad (83)$$

$$\int (m_1 p f_1^* + m_2 p f_2^*) dp = \int (m_1 p f_1^\ell + m_2 p f_2^\ell) dp, \quad (84)$$

$$\int \left(\frac{|p|^2}{2m_1} f_1^* + \frac{|p|^2}{2m_2} f_2^* \right) dp = \int \left(\frac{|p|^2}{2m_1} f_1^\ell + \frac{|p|^2}{2m_2} f_2^\ell \right) dp. \quad (85)$$

Proposition 5.7. *For each $i = 1, 2$, the transport step in the first-order splitting scheme in Section 5.1.1, combined with the space discretization presented in Section 5.2 satisfies the conservation laws*

$$\sum_{i=0}^I \int \mathbf{p}_k f_{k,i}^{\ell+1} dp \Delta x = \sum_{i=0}^I \int \mathbf{p}_k f_{k,i}^* dp \Delta x \quad (86)$$

for periodic or zero boundary conditions.

Since the second-order time-stepping scheme in Section 5.1.2 can be broken into relaxation and transport parts, each of which preserves the conservation of mass, total momentum, and total energy, we can state the following:

Corollary 5.3.1. *For periodic or zero boundary conditions, any combination of temporal and space discretization presented to Sections 5.1 and 5.2, respectively, conserves mass, total momentum and total energy.*

5.3.3 Entropy inequality

We study the entropy behavior for the first-order scheme in Section 5.1.1. Both the relaxation and the transport step dissipate entropy; see Propositions 5.8 and 5.10. Moreover, the minimal entropy is reached for the relaxation step if the distribution functions coincide with the corresponding target functions; see Proposition 5.9.

Proposition 5.8. *Let h_τ given by (11). The relaxation step in the first-order splitting scheme in Section 5.1.1 fulfills the discrete entropy inequality*

$$\int h_\tau(f_1^*) + h_{\tau'}(f_2^*) dp \leq \int h_\tau(f_1^\ell) + h_{\tau'}(f_2^\ell) dp. \quad (87)$$

Proof. By convexity

$$h_{\tau_k}(f_k^\ell) \geq h_{\tau_k}(f_k^*) + h'_{\tau_k}(f_k^*)(f_k^\ell - f_k^*). \quad (88)$$

For $f \geq 0$ ($\tau \in \{-1, 0\}$), respective $0 \leq f < 1$ ($\tau = +1$), the derivative

$$h'_\tau(f) = \log \frac{1}{1 - \tau f} \quad (89)$$

is monotonically increasing such that

$$(h'_\tau(x) - h'_\tau(y))(y - x) \leq 0 \quad (90)$$

for all $x, y \geq 0$ ($\tau \in \{-1, 0\}$) and $0 \leq x, y < 1$ ($\tau = +1$), respectively. Moreover, since

$$h'_{\tau_k}(\mathcal{K}_{kk}^*) = \alpha_k \cdot \mathbf{p}_k, \quad (91)$$

it holds

$$\int h'_{\tau_k}(\mathcal{K}_{kk}^*) \tilde{\nu}_{kk}(\mathcal{K}_{kk}^* - f_k^*) dp = \int \alpha_k \cdot \mathbf{p}_k \tilde{\nu}_{kk}(\mathcal{K}_{kk}^* - f_k^*) dp = 0 \quad (92)$$

which vanishes as the conservation properties are satisfied at the semi-discrete level as well by construction of the scheme. Analogously for the inter-species terms,

$$\begin{aligned} & \int h'_{\tau}(\mathcal{K}_{12}^*) \tilde{\nu}_{12}(\mathcal{K}_{12}^* - f_1^*) dp + \int h'_{\tau'}(\mathcal{K}_{21}^*) \tilde{\nu}_{21}(\mathcal{K}_{21}^* - f_2^*) dp \\ &= \alpha_{12}^0 \int \tilde{\nu}_{12}(\mathcal{K}_{12}^* - f_1^*) dp + \alpha_{21}^0 \int \tilde{\nu}_{21}(\mathcal{K}_{21}^* - f_2^*) dp \\ &+ \left(\frac{\alpha^1}{\alpha^2} \right) \cdot \int (\tilde{\nu}_{12}(\mathcal{K}_{12}^* - f_1^*) \left(\frac{p}{|p|^2} \right) + \tilde{\nu}_{21}(\mathcal{K}_{21}^* - f_2^*) \left(\frac{p}{|p|^2} \right)) dp \\ &= 0. \end{aligned} \quad (93)$$

The implicit step (50) is

$$f_k^* - f_k^\ell = \Delta t \tilde{\nu}_{kk}(\mathcal{K}_{kk}^* - f_k^*) + \Delta t \tilde{\nu}_{kj}(\mathcal{K}_{kj}^* - f_k^*). \quad (94)$$

Using (94) and the convexity of h_τ leads to

$$\begin{aligned} h_{\tau_k}(f_k^*) - h(f_k^\ell) &\leq h'(f_k^*)(f_k^* - f_k^\ell) \\ &\stackrel{(94)}{=} \Delta t h'_{\tau_k}(f_k^*) \tilde{\nu}_{kk}(\mathcal{K}_{kk}^* - f_k^*) + \Delta t h'_\tau(f_k^*) \tilde{\nu}_{kj}(\mathcal{K}_{kj}^* - f_k^*). \end{aligned} \quad (95)$$

Thus after integrating (95) with respect to p and making use of (92) and (93), we obtain

$$\begin{aligned} & \int h_\tau(f_1^*) dp - \int h_\tau(f_1^\ell) dp + \int h_{\tau'}(f_2^*) dp - \int h_{\tau'}(f_2^\ell) dp \\ &\leq \Delta t \int (h'_\tau(f_1^*) - h'_\tau(\mathcal{K}_{11}^*)) \tilde{\nu}_{11}(\mathcal{K}_{11}^* - f_1^*) dp + \Delta t \int (h'_{\tau'}(f_2^*) - h'_{\tau'}(\mathcal{K}_{22}^*)) \tilde{\nu}_{22}(\mathcal{K}_{22}^* - f_2^*) dp \\ &+ \Delta t \int (h'_\tau(f_1^*) - h'_\tau(\mathcal{K}_{12}^*)) \tilde{\nu}_{12}(\mathcal{K}_{12}^* - f_1^*) dp + \Delta t \int (h'_{\tau'}(f_2^*) - h'_{\tau'}(\mathcal{K}_{21}^*)) \tilde{\nu}_{21}(\mathcal{K}_{21}^* - f_2^*) dp \\ &\leq 0. \end{aligned} \quad (96)$$

The last inequality comes by (90). □

Proposition 5.9. *The inequality in Proposition 5.8 is an equality if and only if $f_1^\ell = \mathcal{K}_{12}^\ell$ and $f_2^\ell = \mathcal{K}_{21}^\ell$. In such cases $f_1^* = \mathcal{K}_{12}^*$ and $f_2^* = \mathcal{K}_{21}^*$.*

Proof. The proof works analogously as and can be found in [23]. □

Proposition 5.10. *Let h_τ be given by (11). The transport step in the first-order splitting scheme in Section 5.1.1 combined with the first-order spatial discretization in Section 5.2 fulfills the discrete entropy inequality*

$$\sum_{i=0}^I \left\{ \int h_\tau(f_{1,i}^{\ell+1}) + h_{\tau'}(f_{2,i}^{\ell+1}) dp \right\} \Delta x \leq \sum_{i=0}^I \left\{ \int h_{\tau_1}(f_{1,i}^*) + h_{\tau'}(f_{2,i}^*) dp \right\} \Delta x \quad (97)$$

for periodic or zero boundary conditions, provided that

$$\Delta t \leq \frac{m_k \Delta x}{\max |p^1|}. \quad (98)$$

Proof. We can apply the same proof as in [23] because h_τ is convex. □

We combine the two propositions above and obtain the following:

Corollary 5.3.2. *For periodic or zero boundary conditions, the first-order splitting scheme 5.1.1 combined with the first-order numerical fluxes in Section 5.2 fulfills the discrete entropy inequality*

$$\sum_{i=0}^I \left\{ \int h_\tau(f_{1,i}^{\ell+1}) + h_{\tau'}(f_{2,i}^{\ell+1}) dp \right\} \Delta x \leq \sum_{i=0}^I \left\{ \int h(f_{1,i}^*) + h(f_{2,i}^*) dp \right\} \Delta x \quad (99)$$

provided that

$$\Delta t \leq \frac{m_i \Delta x}{\max |p^1|}. \quad (100)$$

5.4 Momentum discretization

Eventually, we discretize the momentum variable. We center the discrete momenta $p_q = (p_{q_1}^1, p_{q_2}^2, p_{q_3}^3)^\top$, with $q = (q_1, q_2, q_3) \in \mathbb{N}_0^3$, around u_{mix} with the mixture mean velocity

$$u_{\text{mix}} = \frac{p_1 + p_2}{N_1 + N_2} \quad (101)$$

and restrict them to a finite cube. This means, for each component $r \in \{1, 2, 3\}$,

$$p^r \in [m_k u_{\text{mix}}^r - 6m_k v_{\text{th},k}, m_k u_{\text{mix}}^r + 6m_k v_{\text{th},k}] \quad (102)$$

where $v_{\text{th},k} = \sqrt{\frac{T_{\text{mix}}}{m_k}}$ is the thermal velocity of species i and

$$T_{\text{mix}} = \frac{n_1 T_1 + n_2 T_2}{n_1 + n_2} + \frac{1}{3} \frac{N_1 N_2}{N_1 + N_2} \frac{| \frac{P_1}{N_1} - \frac{P_2}{N_2} |^2}{n_1 + n_2} \quad (103)$$

is the mixture temperature. An adequate resolution is ensured by the momentum mesh size $\Delta p_k = 0.25 m_k v_{\text{th},k}$ in each direction, as in [34].

We emphasize the advantage of the multi-species BGK model that it is possible to use different grids for each species/equation. This feature becomes beneficial when the species masses, and hence the thermal speeds, differ significantly.

All momentum integrals are replaced by discrete sums using the trapezoidal rule, i.e.

$$\int (\cdot) dp \approx \sum_q \omega_q (\cdot)_q (\Delta p_k)^3 \quad (104)$$

where $\omega_q = \omega_{q_1} \omega_{q_2} \omega_{q_3}$ are the weights and

$$\omega_{q_p} = \begin{cases} 1 & \text{if } \min(q_p) < q_p < \max(q_p), \\ \frac{1}{2} & \text{else.} \end{cases} \quad (105)$$

We need to distinguish between discrete and continuous moments, especially when determining the discrete local equilibria $\mathcal{K}_{kk,q}$ and $\mathcal{K}_{kj,q}$. Since the minimization of (66) and (67) is solved using a discrete momentum grid and discrete moments $\bar{\mu}_k, \bar{\mu}$ as input, the parameters α_{kk} and α_{kj} are determined such that $\mathcal{K}_{kk,q}$ and $\mathcal{K}_{kj,q}$ have the desired discrete moments. Thus, the conservation and entropy properties are fulfilled at the discrete level. (A similar approach for the standard single-species BGK equation is given in [34].)

Theorem 5.4.1. *Propositions 5.2, 5.3, and 5.8-5.10 all hold true after replacing continuous integrals by their respective quadratures. Additionally, the scheme in Section 5.1.3 satisfies the following conservation properties for $\ell \geq 0$*

$$\sum_{i,q} \omega_q (f_{1,iq}^\ell \mathbf{p}_{1,q} (\Delta p_1)^3 + f_{2,iq}^\ell \mathbf{p}_{2,q} (\Delta p_2)^3) \Delta x \sum_{i,q} \omega_q (f_{1,iq}^0 \mathbf{p}_{1,q} (\Delta p_1)^3 + f_{2,iq}^0 \mathbf{p}_{2,q} (\Delta p_2)^3) \Delta x \quad (106)$$

with $\mathbf{p}_{k,q} = (1, p_q, \frac{|p_q|^2}{2m_k})^\top$ and $f_{k,iq}^\ell \approx f_{k,i}^\ell(p_q)$.

Optimization algorithm The minimization of (66) and (67) is solved by Newton's method which requires the evaluation of the gradients

$$\nabla_{\alpha_k} \varphi_k \approx - \sum_q \omega_q d_{k,q} \tilde{\nu}_{kk,q} \mathcal{K}_{kk,q} \mathbf{p}_{k,q} (\Delta p_k)^3 + \bar{\mu}_k \quad (107)$$

$$\nabla_{\alpha} \varphi \approx - \sum_q \omega_q d_{1,q} \nu_{12,q} \mathcal{K}_{12,q} \mathbf{p}_{12,q} (\Delta p_1)^3 - \sum_q \omega_q d_{2,q} \tilde{\nu}_{21,q} \mathcal{K}_{21,q} \mathbf{p}_{21,q} (\Delta p_2)^3 + \bar{\mu}, \quad (108)$$

and the Hessians

$$\nabla_{\alpha_k}^2 \varphi_k \approx \sum_q \omega_q d_{k,q} \tilde{\nu}_{kk,q} \zeta(\mathcal{K}_{kk,q}, \tau_k) \mathbf{p}_{k,q} \otimes \mathbf{p}_k (\Delta p_k)^3 \quad (109)$$

$$\nabla_{\alpha}^2 \varphi \approx \sum_q \omega_q d_{1,q} \tilde{\nu}_{12,q} \zeta(\mathcal{K}_{12,q}, \tau_1) \mathbf{p}_{12} \otimes \mathbf{p}_{12,q} (\Delta p_1)^3 + \sum_q \omega_q d_{2,q} \tilde{\nu}_{21,q} \zeta(\mathcal{K}_{21,q}, \tau_2) \mathbf{p}_{21} \otimes \mathbf{p}_{21,q} (\Delta p_2)^3 \quad (110)$$

where $\mathbf{p}_{12,q} = (1, 0, p_{1,q}, \frac{|p_{1,q}|^2}{2m_1})^\top$, $\mathbf{p}_{21,q} = (0, \mathbf{p}_{2,q})^\top$ and

$$\zeta(g, \tau) = \begin{cases} g & \text{for } \tau = 0, \\ g^2 e^{-\alpha \cdot \mathbf{p}} & \text{for } \tau = \pm 1. \end{cases} \quad (111)$$

The input data in (64) is computed in a straight-forward way:

$$\bar{\mu}_k \approx \sum_q \omega_q d_{k,q} \tilde{\nu}_{kk,q} G_{k,q} \mathbf{p}_{k,q} (\Delta p_k)^3. \quad (112)$$

Analogously for the input data $\bar{\mu}$ in (65).

6 Numerical results

In this section, we present several numerical tests. We illustrate the properties of our model and demonstrate the properties of our scheme.

6.1 Relaxation in a homogeneous setting

6.1.1 Decay rates and illustration of the schemes' properties

We validate our numerical scheme for quantum particles and verify the decay rates for the mean velocities and kinetic temperatures which are given analytically in Section 3.2.

Initially, we set the distribution functions to Maxwellians

$$f_k = \mathcal{M}[n_k, U_k, T_k, m_k] = \frac{n_k}{(2\pi T_k m_k)^{3/2}} \exp\left(-\frac{|p - m_k U_k|^2}{2T_k m_k}\right) \quad (113)$$

with

$$\begin{aligned} m_1 &= 1.0, & n_1 &= 1.0, & U_1 &= (0.5, 0, 0)^\top, & T_1 &= 1.0, \\ m_2 &= 1.5, & n_2 &= 1.2, & U_2 &= (0.1, 0, 0)^\top, & T_2 &= 0.5. \end{aligned}$$

These initial data are chosen to only illustrate the basic properties of the model and scheme, respectively, but we do not incorporate further physical details (e.g. for a specific quantum regime). The collision frequencies are set to $\tilde{\nu}_{kj} = 1$.

For the simulation, we use a momentum grid with 48^3 nodes and the first-order splitting scheme from Section 5.1.1 with the time step $\Delta t = 0.01$.

We study any combination of classical particles, fermions and bosons. Exemplary for the interactions of fermions with fermions, we illustrate the evolution of the entropy and the entropy dissipation in Figure 1. In Figure 2, we demonstrate the conservation properties where the numerical oscillations in mass, total momentum and total energy are only of the order 10^{-14} .

In Figure 3, we verify the behavior of the mean velocities converging exponentially fast to a common value. The numerical decay rate and the analytical one (19) coincide very well. We only display the rate for the interactions of fermions with fermions because the decay rate is independent of the type of the species.

In Figure 4, we consider the behavior of the temperatures where we distinguish between the kinetic temperatures

$$T_k = \frac{2}{3} \left(\frac{E_k}{N_k} - \frac{1}{2} \frac{|P_k|^2}{m_k N_k^2} \right) \quad (114)$$

and the physical temperatures ϑ_k of the fluid. The latter ones can be calculated via a nonlinear system of equations with the parameters density, fugacity and kinetic temperature [26]. In the first column, we observe that the kinetic temperatures do not converge to a common value whenever a quantum particle is involved. This is also visible in the second column. The numerical and analytical decay rates for the kinetic temperatures coincide very well, and the difference converges to a constant value for quantum particles. Such behavior of the kinetic temperatures for quantum particles comes by an additional term for the decay rates (21) which vanishes for classical-classical interactions, see Remark 5. Additionally, we compare the results to the physical temperatures ϑ_k . Even though the kinetic temperatures behave differently for quantum particles, the physical temperatures converge to a common value in all cases as predicted by the theory.

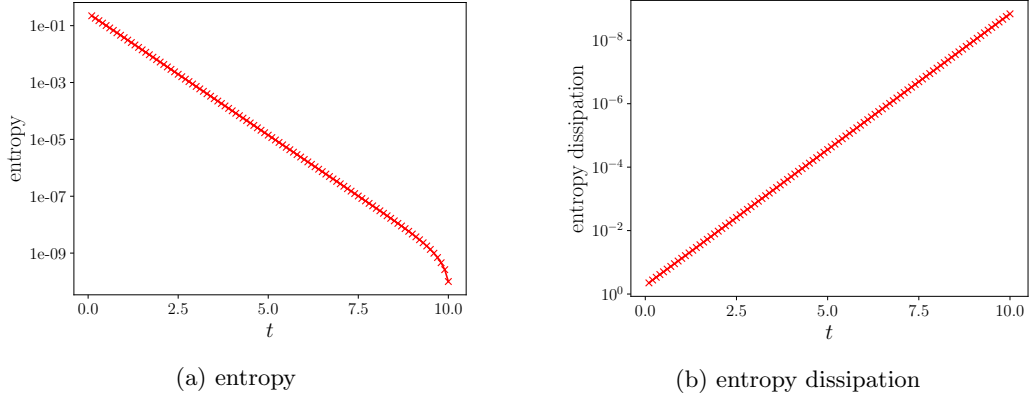


Figure 1: Entropy and entropy dissipation for the test case in Section 6.1.1, exemplary for fermion-fermion interactions. The entropy decays monotonically.

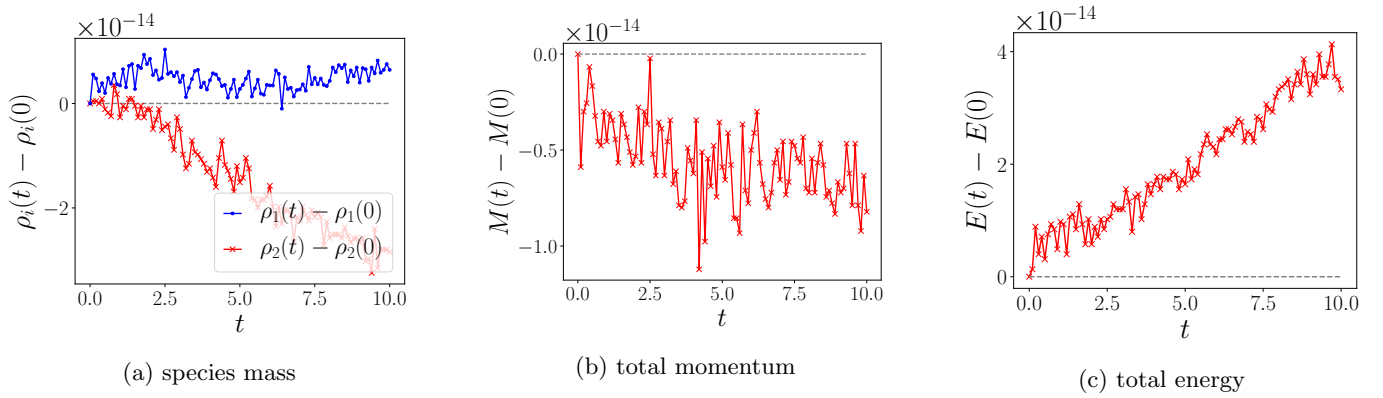


Figure 2: Illustration of the conservation properties for the test case in Section 6.1.1, exemplary for fermion-fermion interactions. The mass densities of each species ($\rho_k = m_k n_k$), the total momentum (M) and total energy (E) have small oscillations of the order of 10^{-14} .

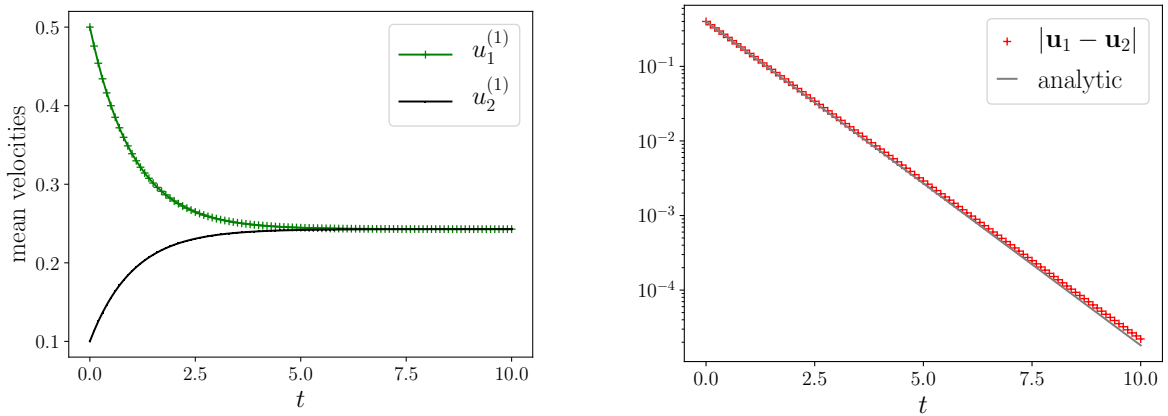


Figure 3: Mean velocities for the test case in Section 6.1.1, exemplary for fermion-fermion interactions. The mean velocities converge exponentially fast to a common value, and the numerical decay rate coincides very well with the analytical one.

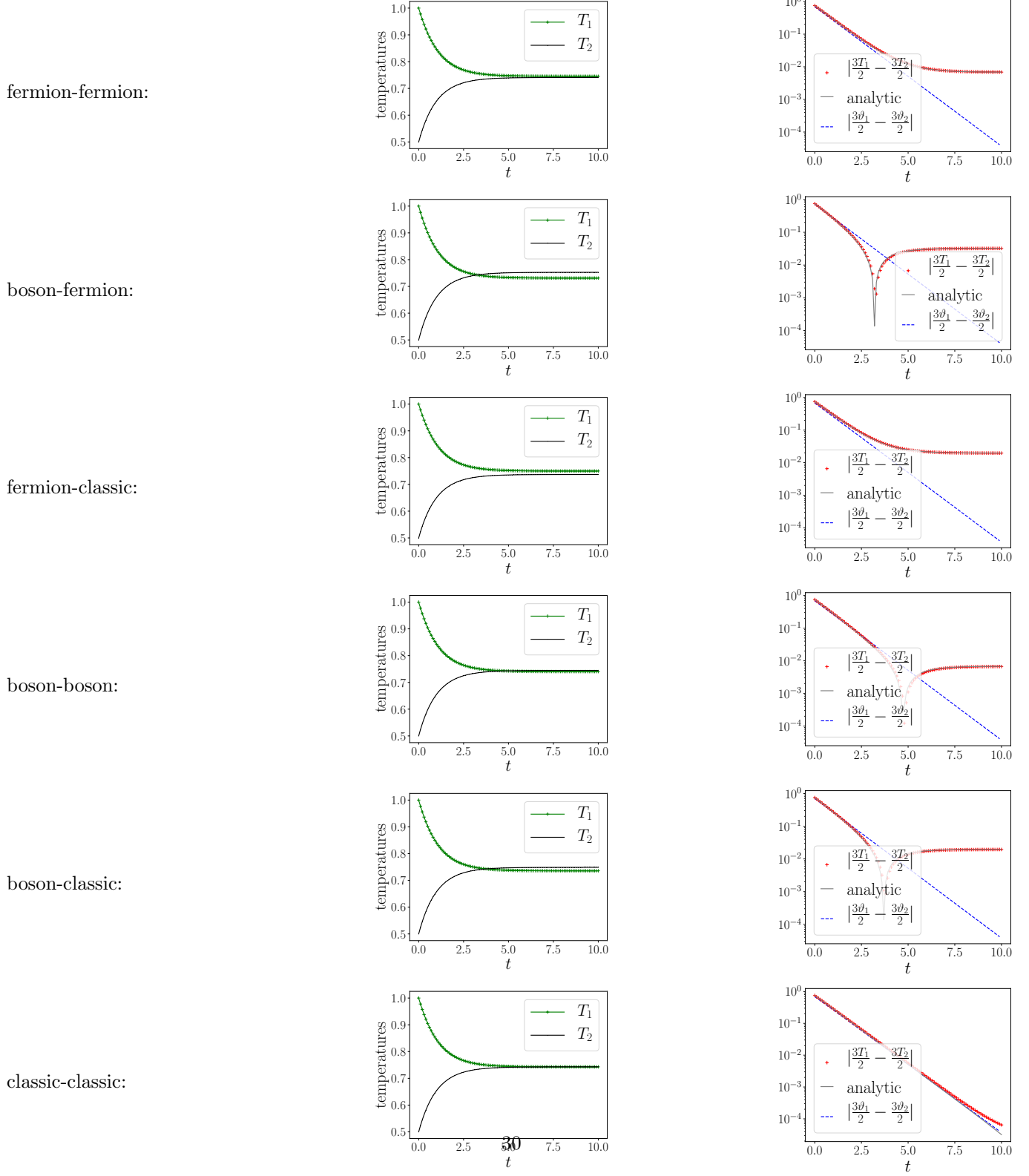


Figure 4: Evolution of the temperatures for the test case in Section 6.1.1. First column: kinetic temperatures T_k ; whenever a quantum particle is involved, the kinetic temperatures do not converge to a common value. Second column: decay rates for kinetic temperatures in logarithmic scale — numerical and analytical values coincide very well. Additionally, the difference between the physical temperatures ϑ_k is displayed which decays exponentially fast, whereas the kinetic temperatures T_k behave differently for quantum particles.

6.1.2 Sulfur-Flourine-electrons test case

We run a space homogeneous, 3-species test case inspired by [24]. In the following, the index S refers to sulfur ions, the index F refers to fluorine ions, and the index e refers to electrons. For convenience, we clarify in the Appendix how the model and the numerical scheme can be extended straight-forwardly to more than two species.

We incorporate collision frequencies $\nu_{kj} = 0.00753 \frac{1}{\text{fs}}$ which are approximately of the same order as those used in [24]. The masses of the species are

$$m_S = 32.07\text{u} - 11m_e, \quad m_F = 19\text{u} - 7m_e, \quad m_e = 9.11 \cdot 10^{-28}\text{g}$$

with the atomic mass $\text{u} = 1.6605 \cdot 10^{-24}\text{g}$. The ions are treated like classical particles and initialized by $f_k = \mathcal{M}[n_k, U_k, T_k, m_k]$ ($k = S, F$) with

$$\begin{aligned} n_S &= 10^{19} \text{ cm}^{-3}, & n_F &= 6 \cdot 10^{19} \text{ cm}^{-3}, \\ U_S &= U_F = 0 \frac{\text{cm}}{\text{s}}, \\ T_S &= T_F = 15 \text{ eV}, \end{aligned}$$

where M is defined in (113). For the electrons, we compare the behavior when they are treated like classical particles to the behavior when they are treated like fermions. In the former case, we initialize $f_e = \mathcal{M}[n_e, U_e, \vartheta_e, m_e]$ with

$$n_e = 53 \cdot 10^{19} \text{ cm}^{-3}, \quad U_e = 0 \frac{\text{cm}}{\text{s}}, \quad \vartheta_e = 100 \text{ eV}.$$

It holds $T_e = \vartheta_e$ for classical particles. In the latter case — electrons being treated as fermions — we initialize the distribution function by a Fermi-Dirac function, but we keep the same macroscopic quantities, i.e.

$$f_e = \left[\frac{(2\pi m_e \vartheta_e)^{3/2}}{\alpha n_e} e^{\frac{|p|^2}{2m_e \vartheta_e}} + 1 \right]^{-1} \quad (115)$$

with the scaling factor $\alpha = 1.061711634$ which leads to the desired $\int f_e dp = n_e$.

We use momentum grids with 48^3 nodes for each species, and we use the second-order IMEX RK scheme from Section 5.1.2 with time step $\Delta t = 0.1 \text{ fs}$.

We illustrate the evolution of the temperatures in Figure 5. For the purely classic test case, the physical and the kinetic temperatures coincide such that the temperature in equilibrium T_{eq} can be precomputed from the initial data [23]:

$$T_{\text{eq}} = T_{\text{mix}}(0) \stackrel{(103)}{=} \frac{n_1 T_1(0) + n_2 T_2(0) + n_3 T_3(0)}{n_1 + n_2 + n_3}. \quad (116)$$

In Figure 5, we observe that all species temperatures converge to that value for the classical simulation. Additionally, we display the results when we consider the electrons to be fermions instead. As predicted by the theory, the physical temperatures converge to a common value. However, the physical temperatures generally differ from the kinetic temperatures in the quantum case. As a consequence, the physical temperature in equilibrium does not equal T_{eq} .

6.2 Sod problem

We run a quantum-kinetic version of the well-known Sod problem [17] in the fluid regime for fermions. As carried out in [14], the limiting equations for the kinetic equations in the fluid regime are the quantum Euler equations.

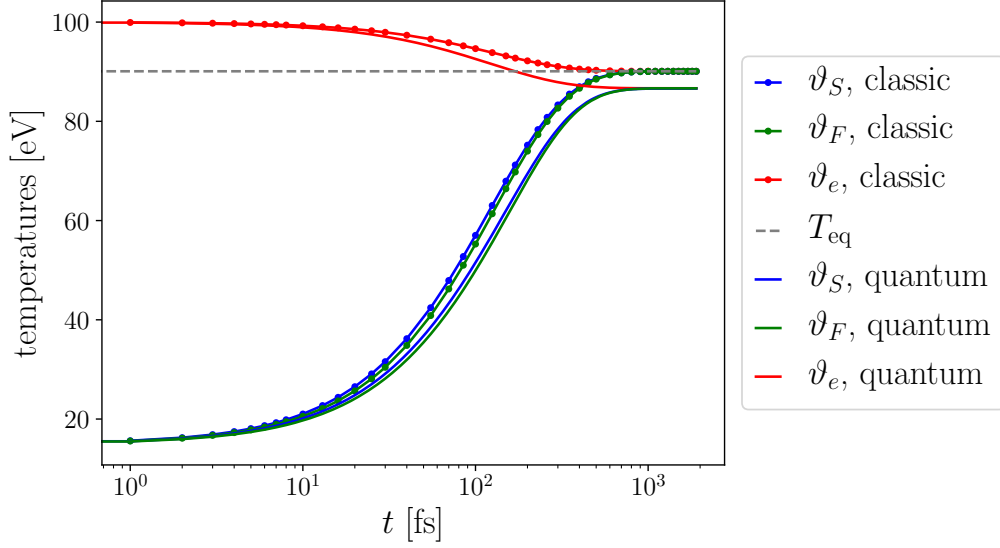


Figure 5: Evolution of the physical temperatures for the Sulfur-Fluorine-electrons quantum test case in Section 6.1.2. When both the ions and the electrons are treated classically (lines with dots), the physical temperatures (which coincide with the kinetic temperatures (114)) converge to the mixture temperature T_{eq} defined in (116). When the electrons are treated like fermions instead, the physical temperatures do converge to a common value as predicted by the theory. However, this value differs from T_{eq} .

We implement a single-species test case with the multi-species model by assuming $m_1 = m_2 = m$, $n_1 = n_2 = n$, $U_1 = U_2 = U$ and $T_1 = T_2 = T$. We set $m = 1$ and use $\tilde{\nu}_{kj} = 2 \cdot 10^4$ for approaching the fluid regime. The initial data is given by $f_1 = f_2 = \mathcal{M}[n, u, T, m]$ where \mathcal{M} is defined in (113) with

$$n = 1, \quad U = 0, \quad T = 1, \quad (117)$$

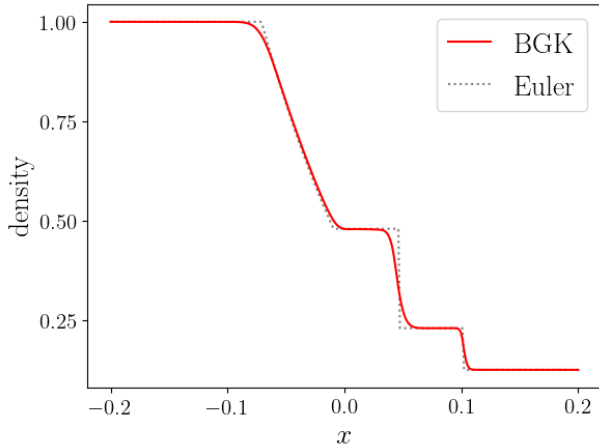
for $x \leq 0$ and

$$n = 0.125, \quad U = 0, \quad T = 0.8 \quad (118)$$

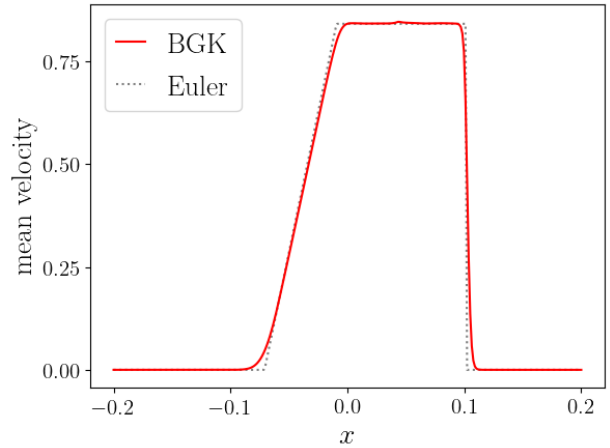
for $x > 0$.

The simulations are run using a velocity grid with 48^3 points and 300 equally spaced cells in x . We use the second-order IMEX Runge-Kutta scheme from Section 5.1.2 combined with the second-order finite volume scheme from Section 5.2.

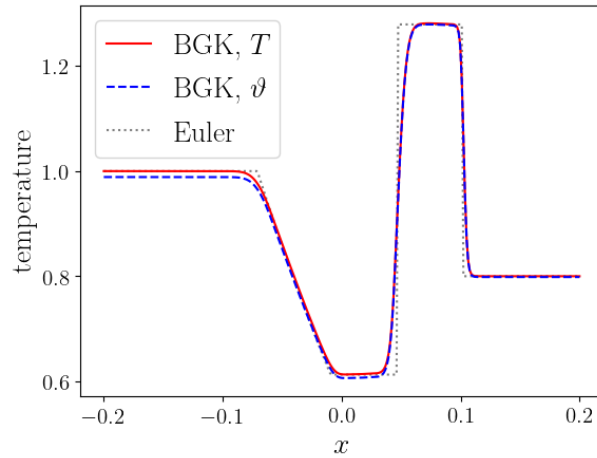
Numerical results of the macroscopic quantities are given in Figure 6. The fluid limit is recovered fairly well by the density n , mean velocity u and kinetic temperature T . We see again that the physical temperature ϑ deviates from the kinetic temperature.



(a) density



(b) mean velocity



(c) temperature

Figure 6: Numerical solution at $t = 0.055$ of the Sod problem in Section 6.2. We show results for a 2-species kinetic simulation for fermions. The solutions for both species are identical; we show only the species 1 results. For reference, the exact solution for the quantum Euler equations is also provided (dotted gray line). The kinetic solution recovers the fluid limit fairly well.

7 Appendix

The two-species model can be extended to a system of N -species which undergo binary interactions. For ease in notation, we illustrate here the 3-species case. Each distribution function f_k , $k = 1, \dots, 3$, represents the solution to

$$\partial_t f_k + \frac{p}{m_k} \cdot \nabla_x f_k = \tilde{\nu}_{k1}(\mathcal{K}_{k1} - f_k) + \tilde{\nu}_{k2}(\mathcal{K}_{k2} - f_k) + \tilde{\nu}_{k3}(\mathcal{K}_{k3} - f_k) \quad (119)$$

with $\tilde{\nu}_{kj} = \nu_{kj} n_j$. Since we still consider only binary interactions, the properties in section 2 and 3.1 are still satisfied.

The presented numerical scheme is based on the general implicit solver in Section 5.1.3. Since the transport operators act only on the individual species, we focus on and shortly illustrate the scheme of the relaxation process.

As above, we write the implicit updates of the distribution functions in a generic steady state form

$$f_k = d_k G_k + d_k \gamma \Delta t (\tilde{\nu}_{kk} \mathcal{K}_{kk, \tau_k} + \tilde{\nu}_{kj} \mathcal{K}_{kj, \tau_j} + \tilde{\nu}_{kl} \mathcal{K}_{kl, \tau_l}) \quad (120)$$

for $k, j, l \in \{1, 2, 3\}$, each of k, j, l distinct, where \mathcal{K}_{kk, τ_k} , \mathcal{K}_{kj, τ_j} and \mathcal{K}_{kl, τ_l} are the unique attractors associated to f_k ,

$$d_k = \frac{1}{1 + \gamma \Delta t (\tilde{\nu}_{kk} + \tilde{\nu}_{kj} + \tilde{\nu}_{kl})}, \quad (121)$$

and G_k is a known function. When we can express \mathcal{K}_{kk} , \mathcal{K}_{kj} and \mathcal{K}_{kl} as functions of G_k , G_j and G_l , (120) provides an explicit update formula for f_k .

We apply the conservation properties to (120). An analogous calculation as in the 2-species case leads to a set of constraints to determine the attractors from the given data:

$$\begin{aligned} & \int d_1 (\tilde{\nu}_{11} \mathcal{K}_{11, \tau_1} + \tilde{\nu}_{12} \mathcal{K}_{12, \tau_1} + \tilde{\nu}_{13} \mathcal{K}_{13, \tau_1}) \mathbf{p}_1 dp + \int d_2 (\tilde{\nu}_{21} \mathcal{K}_{21, \tau_2} + \tilde{\nu}_{22} \mathcal{K}_{22, \tau_2} + \tilde{\nu}_{23} \mathcal{K}_{23, \tau_2}) \mathbf{p}_2 dp \\ & + \int d_3 (\tilde{\nu}_{31} \mathcal{K}_{31, \tau_3} + \tilde{\nu}_{32} \mathcal{K}_{32, \tau_3} + \tilde{\nu}_{33} \mathcal{K}_{33, \tau_3}) \mathbf{p}_3 dp \\ & = \int d_1 (\tilde{\nu}_{11} + \tilde{\nu}_{12} + \tilde{\nu}_{13}) G_1 \mathbf{p}_1 dp + \int d_2 (\tilde{\nu}_{21} + \tilde{\nu}_{22} + \tilde{\nu}_{23}) G_2 \mathbf{p}_2 dp + \int d_3 (\tilde{\nu}_{31} + \tilde{\nu}_{32} + \tilde{\nu}_{33}) G_3 \mathbf{p}_3 dp. \end{aligned} \quad (122)$$

These constraints (122) represent first-order optimality conditions associated to the minimization of the convex function

$$\varphi_{\text{tot}}(\alpha_1, \alpha_2, \alpha_3, \alpha_{12}, \alpha_{13}, \alpha_{23}) = \varphi_1(\alpha_1) + \varphi_2(\alpha_2) + \varphi_3(\alpha_3) + \varphi(\alpha_{12}) + \varphi(\alpha_{13}) + \varphi(\alpha_{23})$$

with

$$\varphi_k(\alpha_k) = \int d_k \tilde{\nu}_{kk} w[\mathcal{K}_{kk, \tau_k}] dp + \mu_{kk} \cdot \alpha_k$$

and

$$\varphi(\alpha_{kj}) = \int (d_k \tilde{\nu}_{kj} w[\mathcal{K}_{kj, \tau_k}] + d_j \tilde{\nu}_{jk} w[\mathcal{K}_{jk, \tau_j}]) dp + \mu_{kj} \cdot \alpha_{kj},$$

where

$$w[\mathcal{K}_{kj, \tau_k}] = \frac{\log(1 - \tau_k \mathcal{K}_{kj, \tau_k})}{\tau_k} = \begin{cases} -\mathcal{K}_{kj, \tau_k} & \text{for } \tau_k = 0, \\ \log(1 - \mathcal{K}_{kj, 1}) & \text{for } \tau_k = +1, \\ -\log(1 + \mathcal{K}_{kj, -1}) & \text{for } \tau_k = -1. \end{cases}$$

Moreover, $\alpha_k = (\alpha_k^0, \alpha_k^1, \alpha_k^2)^\top$;

$$\mu_{kk} = \begin{pmatrix} \mu_{kk}^0 \\ \mu_{kk}^1 \\ \mu_{kk}^2 \end{pmatrix} = \int d_k \tilde{\nu}_{kk} G_k \mathbf{P}_k dp$$

for $k = 1, 2, 3$; for $k \neq j$: $\alpha_{kj} = (\alpha_{kj}^0, \alpha_{kj}^1, \alpha_{kj}^2)^\top$; and

$$\mu_{kj} = \begin{pmatrix} \mu_{kj}^0 \\ \mu_{kj}^1 \\ \mu_{kj}^2 \end{pmatrix} = \int \left[\begin{pmatrix} 1 \\ 0 \\ p \\ \frac{|p|^2}{2m_k} \end{pmatrix} d_k \nu_{kj} G_k + \begin{pmatrix} 0 \\ 1 \\ p \\ \frac{|p|^2}{2m_j} \end{pmatrix} d_j \nu_{jk} G_j \right] dp.$$

8 Acknowledgements

Marlies Pirner was funded by the Deutsche Forschungsgemeinschaft (DFG, German Research Foundation) under Germany's Excellence Strategy EXC 2044-390685587, Mathematics Münster: Dynamics–Geometry–Structure, by the Alexander von Humboldt foundation and the German Science Foundation DFG (grant no. PI 1501/2-1).

References

- [1] P. Andries, K. Aoki and B. Perthame, A consistent BGK-type model for gas mixtures, *Journal of Statistical Physics* 106 (2002) 993-1018
- [2] Ascher, U.M., Ruuth, S.J., Spiteri, R.J.: Implicit-explicit Runge-Kutta methods for time-dependent partial differential equations. *Applied Numerical Mathematics* **25** (1997), no. 2, 151-167
- [3] Ashcroft, N. W.: *Solid State Physic*. Thomson Press, 2003.
- [4] Bae, G. C., Yun, S. B. (2020). Quantum BGK Model near a Global Fermi–Dirac Distribution. *SIAM Journal on Mathematical Analysis*, 52(3), 2313-2352.
- [5] Bae, G. C., Klingenberg, C., Pirner, M., Yun, S. B. (2019). BGK model of the multi-species Uehling Uhlenbeck equation. arXiv preprint arXiv:1912.01677.
- [6] Bae, G.-C., Yun, S.-B.: Stationary quantum BGK model for bosons and fermions in a bounded interval. *J. Stat. Phys.* **178** (2020), no. 4, 845-868.
- [7] Bae, G. C., Klingenberg, C., Pirner, M., Yun, S. B.: BGK model of the multi-species Uehling-Uhlenbeck equation. *Kinet. Relat. Models* (2021), no.1, 25–44.
- [8] Bae, G. C., Klingenberg, C., Pirner, M., Yun, S. B.: BGK model for two-component gases near a global Maxwellian. *SIAM J. Math. Anal.* 55 (2023), no.2, 1007–1047.
- [9] Bae, G. C., Klingenberg, C., Pirner, M., Yun, S. B.: BGK model for two-component gases near a global Maxwellian. *SIAM Journal of Mathematical Analysis* 55 (2), 2023

- [10] Bobylev, A. V., Bisi, M., Groppi, M., Spiga, G., Potapenko, I. F. (2018). A general consistent BGK model for gas mixtures. *Kinetic and Related Models*, 11(6).
- [11] S. Brull, V. Pavan and J. Schneider, *Derivation of a BGK model for mixtures*, *European Journal of Mechanics B/Fluids*, 33 (2012) 74-86
- [12] Escobedo, M., Mischler, S., Valle, M. A.: Entropy maximisation problem for quantum relativistic particles. *Bull. Soc. Math. France.* **133** (2005) no. 1, 87-120.
- [13] Feng, D., Jin, G.: *Introduction to Condensed Matter Physics*, World Scientific Publishing Company, 2005.
- [14] Francis Filbet, Jingwei Hu, Shi Jin (2012): A numerical scheme for the quantum Boltzmann equation with stiff collision terms. *ESAIM: M2AN* 46 (2) 443-463, DOI: 10.1051/m2an/2011051
- [15] Gamba, Irene M and Haack, Jeffrey R and Hauck, Cory D and Hu, Jingwei, A fast spectral method for the Boltzmann collision operator with general collision kernels, *SIAM Journal on Scientific Computing* 39 (4), pp. B658–B674 (2017)
- [16] Gamba, Irene M and Tharkabhushanam, Sri Harsha, Spectral-Lagrangian methods for collisional models of non-equilibrium statistical states, *Journal of Computational Physics* 228 (6), pp. 2012–2036 (2009)
- [17] Gary A. Sod: A survey of several finite difference methods for systems of nonlinear hyperbolic conservation laws. *Journal of Computational Physics* **27** (1978), no. 1, 1–31
- [18] V. Garzó, A. Santos and J. J. Brey, *A kinetic model for a multicomponent gas* *Physics of Fluids*, 1 (1989) 380-383
- [19] J. Greene, Improved Bhatnagar-Gross-Krook model of electron-ion collisions. *Phys. Fluids* 16, 2022– 2023 (1973)
- [20] E. P. Gross and M. Krook, *Model for collision processes in gases: small-amplitude oscillations of charged two-component systems*, *Physical Review* 3 (1956) 593
- [21] J. R. Haack, C.D. Haack, and M.S.Murillo . A conservative, entropic multispecies BGK model. *Journal of Statistical Physics*, 168 (2017), 826-856.
- [22] Haack, J., Hauck, C., Klingenberg, C., Pirner, M., Warnecke, S.: A consistent BGK model with velocity-dependent collision frequency for gas mixtures. *J. Stat. Phys.* **184** (2021), no. 31.
- [23] Haack, J., Hauck, C., Klingenberg, C., Pirner, M., Warnecke, S. (2022). Numerical schemes for multi-species BGK equations with velocity-dependent collision frequency. submitted. arXiv preprint arXiv:2202.05652.
- [24] Haack, J., Hauck, C., Murillo, M.: A conservative, entropic multispecies BGK model. *J. Stat. Phys.* **168** (2017), no. 4, 826–856
- [25] B. Hamel, *Kinetic model for binary gas mixtures*, *Physics of Fluids* 8 (1965) 418-425
- [26] Hu, J., Jin, S. (2011). On kinetic flux vector splitting schemes for quantum Euler equations. *Kinetic and Related Models*.
- [27] Jüngel, A.: *Transport equations for semiconductors*. *Lecture Notes in Physics*, 773. Springer-Verlag, Berlin, 2009.
- [28] C. Klingenberg, M.Pirner, G.Puppo, A consistent kinetic model for a two-component mixture with an application to plasma, *Kinetic and related Models* 10 (2017) 445-465

- [29] Lu, X.: A Modified Boltzmann Equation for Bose-Einstein Particles: Isotropic Solutions and Long-Time Behavior. *J. Statist. Phys.* **98** (2000), no. 5-6, 1335–1394.
- [30] Lu, X.: On Spatially Homogeneous Solutions of a Modified Boltzmann Equation for Fermi-Dirac Particles. *J. Statist. Phys.* **105** (2001), no. 1-2, 353–388.
- [31] Madelung, O.: Introduction to solid-state theory. Vol. 2. Springer Science and Business Media, 2012.
- [32] Markowich, P. A., Ringhofer, C. A., Schmeiser, C. : Semiconductor equations. Springer-Verlag, Vienna, 1990.
- [33] Mieussens, Luc and Struchtrup, Henning. Numerical comparison of Bhatnagar–Gross–Krook models with proper Prandtl number. *Physics of Fluids*. 16. 10.1063/1.1758217 (2004)
- [34] Mieussens, Luc. Discrete velocity model and implicit scheme for the BGK equation of rarefied gas dynamics; *Mathematical Models and Methods in Applied Sciences*, Vol. 10, No. 08 (2000): 1121-1149
- [35] Mouhot, Clément and Pareschi, Lorenzo, Fast algorithms for computing the Boltzmann collision operator, *Mathematics of computation* 75, 256, pp. 1833–1852 (2006)
- [36] Pareschi, Lorenzo and Russo, Giovanni, Numerical solution of the Boltzmann equation I: Spectrally accurate approximation of the collision operator, *SIAM journal on numerical analysis* 37, 4, pp. 1217–1245 (2000)
- [37] Reinhard, P. G., Suraud, E.: A quantum relaxation-time approximation for finite fermion systems. *Annals of Physics* **354** (2015), 183–202.
- [38] V. Sofonea and R. Sekerka, *BGK models for diffusion in isothermal binary fluid systems*, *Physica*, 3 (2001), 494-520
- [39] Uehling, E. A., Uhlenbeck, G. E.: Transport phenomena in einstein-bose and fermi-dirac gases. i. *Physical Review*, 43 (1933), no. 7, 552.
- [40] Uehling, E. A.: Transport phenomena in einstein-bose and fermi-dirac gases. ii. *Physical Review*, 46 (1934), no. 10, 917.